iScience

CellPress
OPEN ACCESS

Article

Contact-mediated algicidal mechanism of *Vibrio coralliirubri* ACE001 against the harmful alga Karenia mikimotoi

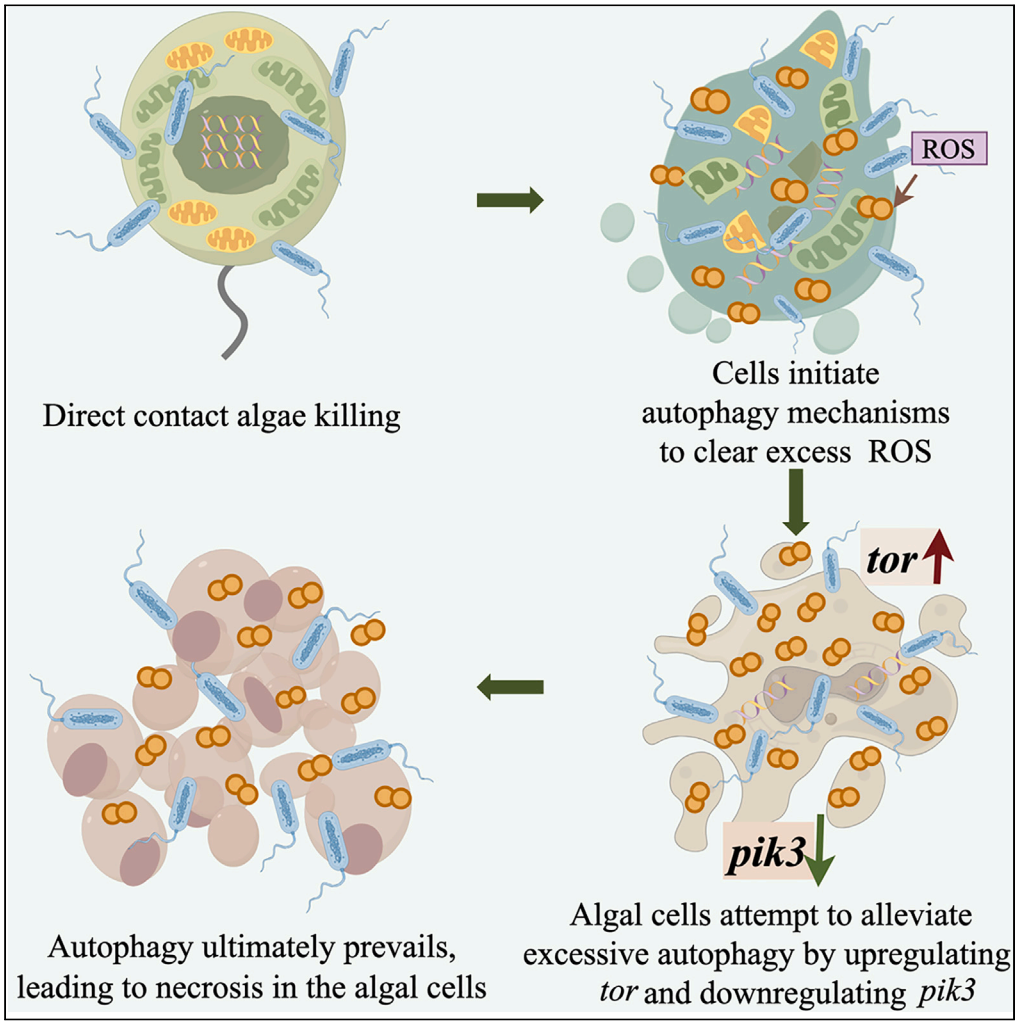

Jiaying Yu, Wei Xu, Jiaxin Wang, Qiancheng Gao, Lijun Xiu, Qingpi Yan, Lixing Huang

yanqp@jmu.edu.cn

Highlights

V. coralliirubri ACE001 exhibits contact-dependent algicidal effects against *K. mikimotoi*

ACE001's attraction to *K. mikimotoi* cell membranes enhancing algicidal activity

Sec system is crucial for algicidal action

Yu et al., iScience 27, 111254
November 15, 2024
https://doi.org/10.1016/j.isci.2024.111254

iScience

CellPress
OPEN ACCESS

Article

Contact-mediated algicidal mechanism of *Vibrio coralliirubri* ACE001 against the harmful alga Karenia mikimotoi

Jiaying Yu,[1,4] Wei Xu,[2,4] Jiaxin Wang,[1] Qiancheng Gao,[1] Lijun Xiu,[1] Qingpi Yan,[1,3] and Lixing Huang[1,5,*]

SUMMARY

***Karenia mikimotoi* is a harmful algal bloom (HAB) species that poses a significant threat to marine ecosystems due to its hemolytic toxins. This study isolated *Vibrio coralliirubri* (ACE001), which demonstrated contact-dependent algicidal effects against *K. mikimotoi*. Chemotaxis assays revealed ACE001's strong attraction to *K. mikimotoi* cell membranes, indicating the importance of chemotaxis. ACE001 caused a significant decrease in Chlorophyll *a* and an increase in reactive oxygen species (ROS), indicating oxidative stress. Scanning electron microscopy showed ACE001 adheres to and penetrates *K. mikimotoi*, leading to cell rupture. Dual RNA-seq revealed suppression of the type VI secretion system (T6SS) and the upregulation of the Sec secretion system, particularly the *yidC* and *secY* genes. Mutant strains lacking these genes exhibited reduced algicidal activity. This study provides the evidence of a *Vibrio* species with algicidal activity against *K. mikimotoi*, offering insights into its algicidal mechanisms.**

INTRODUCTION

In recent decades, the proliferation of harmful algal blooms (HABs) has emerged as a significant threat to marine ecosystems globally.[1] For aquatic organisms, HABs jeopardize their safety, while for humans, they pose health risks and hinder the economic development of marine-dependent industries. Numerous strategies have been implemented to manage HABs to date,[2,3] including physical,[4] chemical,[5] and microbial control measures. However, the efficacy of physical and chemical methods is often constrained by their high costs and potential side effects. Consequently, there has been a growing interest in exploring microbial agents and the interactions between bacteria and algae for HAB mitigation. Notably, the identification and utilization of natural algicidal bacterial resources present a promising alternative. This strategy harnesses the inherent capabilities of specific bacterial strains to target and neutralize harmful algal species, offering a more sustainable and environmentally friendly solution compared to conventional methods.[6,7] It is noteworthy to highlight the exemplary research conducted by Grasso, Christopher, and colleagues in the United States on the "DinoSHIELD" project, involving the slow release of immobilized algicidal bacteria embedded within an alginate gel matrix. This innovative approach has progressed to the mesoscale experimental phase.[8]

In fact, the relationship between bacteria and algae in aquatic ecosystems is intricate and dynamic, exhibiting a spectrum of interactions ranging from mutualistic to symbiotic and parasitic relationships.[9] Among these, algicidal bacteria have been identified to exert inhibitory or lytic effects on harmful algal species. Notably, the genera within the family *Pseudoalteromonadaceae* and *Alteromonadaceae* have been implicated in algicidal activities,[10] suggesting their potential role in the management of HABs. The specificity of algicidal bacteria is evident, as different strains demonstrate varying effects on distinct algal species,[11] this specificity underscores the complexity of bacterio-algal interactions and highlights the importance of understanding these dynamics for the development of targeted HAB control strategies. For instance, FDHY-03 isolated from *Prorocentrum donghaiense* by Shi et al.[12] can secrete algae-killing substances and cause organism damage to *P. donghaiense*. It was found by scanning electron microscope (SEM) that the algae-lysing active substances released by FDHY-03 can destroy the integrity of algae cell membrane and significantly change the internal structure of algae cells, resulting in a large number of algae contents being released. The bacterial strain Y42, belonging to the *Paracoccus*, was isolated from the bloom-forming alga *Prorocentrum donghaiense* in the East China Sea. Y42 has been shown to lyse *P. donghaiense* and exhibit algicidal activity against several other algal species, including *Alexandrium minutum*, *Skeletonema costatum*, and *Sargassum conelii*, indicating a primary specificity for the class Dinophyceae.[13] Additionally, a strain S03 from the Cytophaga-Flavobacteria-Bacteroidetes (CFB) group, isolated by Roth, P. B., demonstrated contact-mediated algicidal activity, while strain 41-DBG2 exhibited indirect algicidal effects, with both showing activity against dinoflagellates and diatoms.[14] Hare et al. conducted a screening of bacteria from red tide waters, identifying *Shewanella* IRI-160, a member of the

[1]State Key Laboratory of Mariculture Breeding, Fisheries college of Jimei university, Xiamen, Fujian, P.R. China
[2]Center for Research and Development, Xiamen Treatgut Biotechnology Co., Ltd., Xiamen, China
[3]Senior author
[4]These authors contributed equally
[5]Lead contact
*Correspondence: yanqp@jmu.edu.cn
https://doi.org/10.1016/j.isci.2024.111254

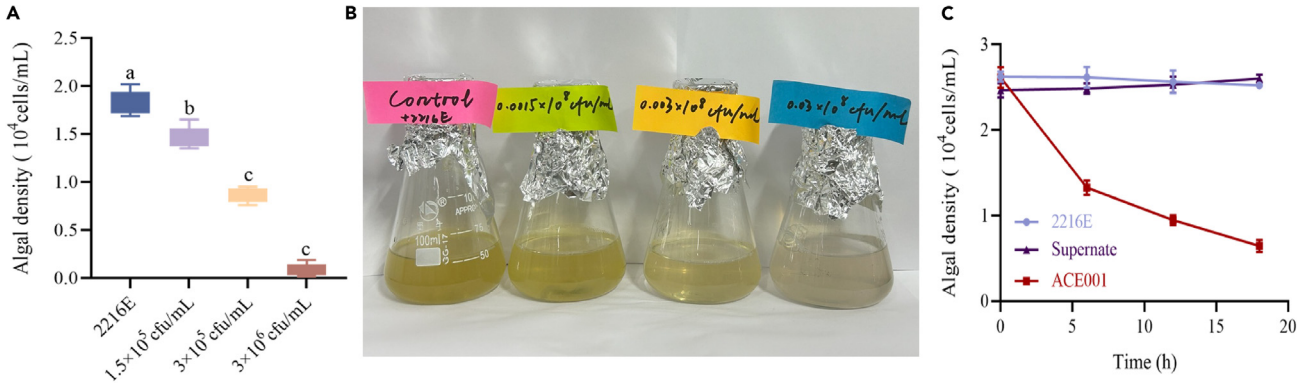

Figure 1. ACE001 exhibits highly effective algicidal activity against *K. mikimotoi*

(A) Effects of varying concentrations of ACE001 on algal cell counts after 24 h of co-culture. Data are expressed as mean ± standard deviation, with distinct letters indicating statistically significant differences among groups.

(B) Algal solution after 24 h of co-culture of ACE001 with *K. mikimotoi* at different ACE001 concentrations.

(C) Algal cell counts following treatment with ACE001 over varying time periods.

Gammaproteobacteria, which was found to inhibit multiple dinoflagellate species without adversely affecting common non-dinoflagellate species such as diatoms and green algae in estuarine environments.[15] Furthermore, algicidal bacteria within the same genus can have varying effects on different phytoplankton species.[16] The genus *Alteromonas* has been reported to possess algicidal activity against a range of phytoplankton species. Zheng et al. isolated several strains of *Alteromonas*, which displayed algicidal activity against *K. mikimotoi*,[17] whereas the strain FDHY-03 from the same genus did not exhibit such effects, highlighting the specificity of these bacteria toward phytoplankton. However, the intrinsic principles of bacterial specificity in algicidal activity and the physiological and molecular mechanisms underlying the process of algal cell death remain to be fully elucidated.

K. mikimotoi is recognized as one of the primary bloom-forming species globally, with the potential to cause massive marine mortality during HAB events, inflicting severe damage on the aquaculture industry and resulting in substantial economic losses.[18] At present, numerous studies have focused on bacteria that inhibit the growth of *K. mikimotoi*,[16] such as the strain FDHY-M22 isolated by Shi et al.[19] from red tide seawater. It has been discovered that the supernatant of this bacterium can act on the cell wall of *K. mikimotoi* and exert a lytic effect on it. After drying the bacterial culture to produce a powder, the algicidal rate of this powder has been tested, providing a strategy for the application of red tide control.

In this study, we isolated a strain of *V. coralliirubri*, designated ACE001, from the Dongshan sea area of Fujian Province following a harmful algal bloom (HAB) outbreak. This strain exhibited contact-mediated algicidal activity against *K. mikimotoi*. Building on our analysis of ACE001's algicidal behavior, we employed genomic sequencing, dual RNA sequencing analysis, and gene knockout techniques to elucidate the molecular mechanisms underlying its algicidal action. Our findings confirm that ACE001 can inject effector molecules into *K. mikimotoi* cells via the Sec secretion system, resulting in a significant increase in reactive oxygen species (ROS) levels and ultimately inducing cell death through an autophagic pathway. This research not only clarifies the principles governing ACE001's algicidal activity but also provides a theoretical foundation for the further development and application of this bacterial strain in the mitigation of HABs.

RESULTS

Identification of *V. coralliirubri* ACE001

The strain ACE001, isolated from seawater during a red tide event, was identified as *V. coralliirubri* based on 16S rDNA gene sequence analysis utilizing the EzTaxon-e database. Phylogenetic analysis indicated a close relationship with *Vibrio anguillarum* and *Vibrio vulnificus* (Figure S1A). Scanning electron microscopy (SEM) observations revealed that ACE001 possesses a short, coccobacillary morphology characterized by a single polar flagellum (Figure S1B). Culturing ACE001 on 2216E agar plates produced colonies that exhibited yellow pigmentation and a circular form with smooth edges (Figure S1C).

Contact algal killing effect of ACE001 on *K. mikimotoi*

The algicidal activity of ACE001 was determined by co-culturing it with *K. mikimotoi* at three different bacterial concentrations (Figure 1A), followed by cell counting after 24 h of incubation. A significant reduction in algal cell numbers was observed in the treatment group with ACE001 at a concentration of 3×10^6 cfu/mL, achieving an algal lysis rate of 95.2%. At concentrations of 3×10^5 cfu/mL and 1.5×10^5 cfu/mL, the lysis rates were 52.6% and 20.4%, respectively (Figure 1B). For subsequent experiments, we selected a bacterial concentration of 3×10^5 cfu/mL for artificial infection assays. To explore the mode of algicidal action of ACE001, we collected sterile supernatant from ACE001 cultures through centrifugation and filtration and added it to *K. mikimotoi* cultures. The results showed that the sterile supernatant did not exhibit significant algicidal activity (Figure 1C), indicating that ACE001 does not cause algal cell death through an indirect dissolution

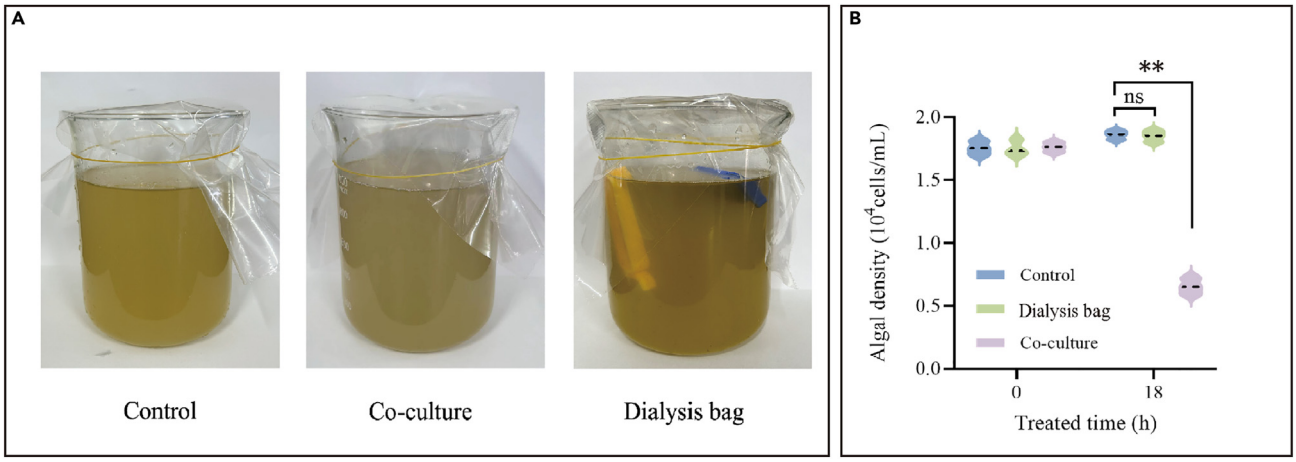

Figure 2. The algicidal effect of ACE001 on *K. mikimotoi* is contingent upon direct contact

(A) Co-culture of the algal suspension with a dialysis bag over an 18-h period.

(B) Quantification of algal cells after 18 h of co-culture with the dialysis bag. Data are presented as mean ± standard deviation. Statistical significance is indicated by $p < 0.01$.

mechanism and confirming that the substance responsible for algal cell death is not present in the supernatant. To further investigate the mode of algicidal action of ACE001, we used dialysis bags to separate ACE001 from the algal cells and observed the algicidal effect. When ACE001 was isolated from the algal cells using dialysis bags, *K. mikimotoi* grew normally, and ACE001 exhibited negligible algicidal effect (Figure 2). These findings suggest that the algicidal activity of ACE001 requires direct contact with the algal cells.

Chemotaxis analysis of ACE001 toward *K. mikimotoi*

Given the contact-mediated algicidal mode of action of ACE001, we hypothesized that ACE001 may utilize chemotactic motility to approach *K. mikimotoi*. To evaluate this hypothesis, we assessed the chemotactic capability of ACE001 toward *K. mikimotoi* using a swarm motility assay. The results revealed distinct chemotactic rings on the plates when *K. mikimotoi* cultures were employed as chemoattractants, indicating that ACE001 exhibits directed motility toward *K. mikimotoi*, potentially to optimize the utilization of organic nutrients secreted by algal cells. To further investigate the underlying mechanisms of ACE001's directed motility toward *K. mikimotoi*, we extracted various cellular fractions from *K. mikimotoi* and co-cultured them with ACE001 on swarm plates. The findings demonstrated that ACE001 displays chemotaxis toward intact algal cells as well as toward cellular organelles, nuclei, and membranes of *K. mikimotoi*, but not toward the cytoplasm (Figure 3).

Morphological and structural changes of *K. mikimotoi* during the process of algal killing

We employed SEM to observe the morphological changes in *K. mikimotoi* cells during the algicidal process. The control group of algal cells exhibited intact morphology with clearly visible, thick thecal plates. Upon the addition of ACE001 to the *K. mikimotoi* culture, distinct interactions between ACE001 and the algal cells were observed. The ACE001 was seen adhering to the surface of the algal cells and, in some instances, penetrating the cells. Over time, the algal cells began to lyse, losing their intact cellular structure, with severe damage to the cell membrane and cell wall, resulting in the leakage of cellular contents and eventual cell death (Figure 4A). This indicates that ACE001 can cause severe disruption to the cellular morphology and structure of *K. mikimotoi*, leading to cell death. We utilized DAPI staining and confocal microscopy to examine the infection process. In the control group, normal algal cells displayed uniform and bright blue DAPI fluorescence. After 6 h of co-culture with ACE001, the blue fluorescence became faint and diffuse, with bright-field images showing direct bacterial contact with algal cells, causing cell rupture and loss of integrity. At 12 h post co-culture, the blue fluorescence was even weaker and more diffuse than at 6 h, with the nuclear structure completely destroyed and appearing fragmented, indicating cell lysis and death (Figure 4B). During the later stages of co-culture (18 h), staining with Hoechst 33342 and observation under confocal microscopy revealed that the algal cell nuclei were barely visible, suggesting that the nucleic material within the cells had been completely degraded. In contrast, the bacteria, which had invaded the algal cells, exhibited clear and bright blue fluorescence, indicating active bacterial activity (Figure 4C). Based on these observations, we hypothesize that the bacteria ACE001 can disrupt the integrity of the cell membrane of *K. mikimotoi*, leading to its damage, while also damaging the nucleus and organelles, resulting in typical necrotic features such as nuclear fragmentation, dissolution, and organelle disintegration. Collectively, these phenomena lead us to speculate that the algal cells may undergo necrosis under the stress imposed by ACE001.

Changes in pigment content within algal cells during co-cultivation with ACE001

Pigment content is a critical indicator for evaluating the health status of algae. With this in mind, we measured the concentrations of Chlorophyll *a* in *K. mikimotoi* during the infection process. We co-cultured ACE001 at a concentration of 3×10^5 cfu/mL with *K. mikimotoi* and

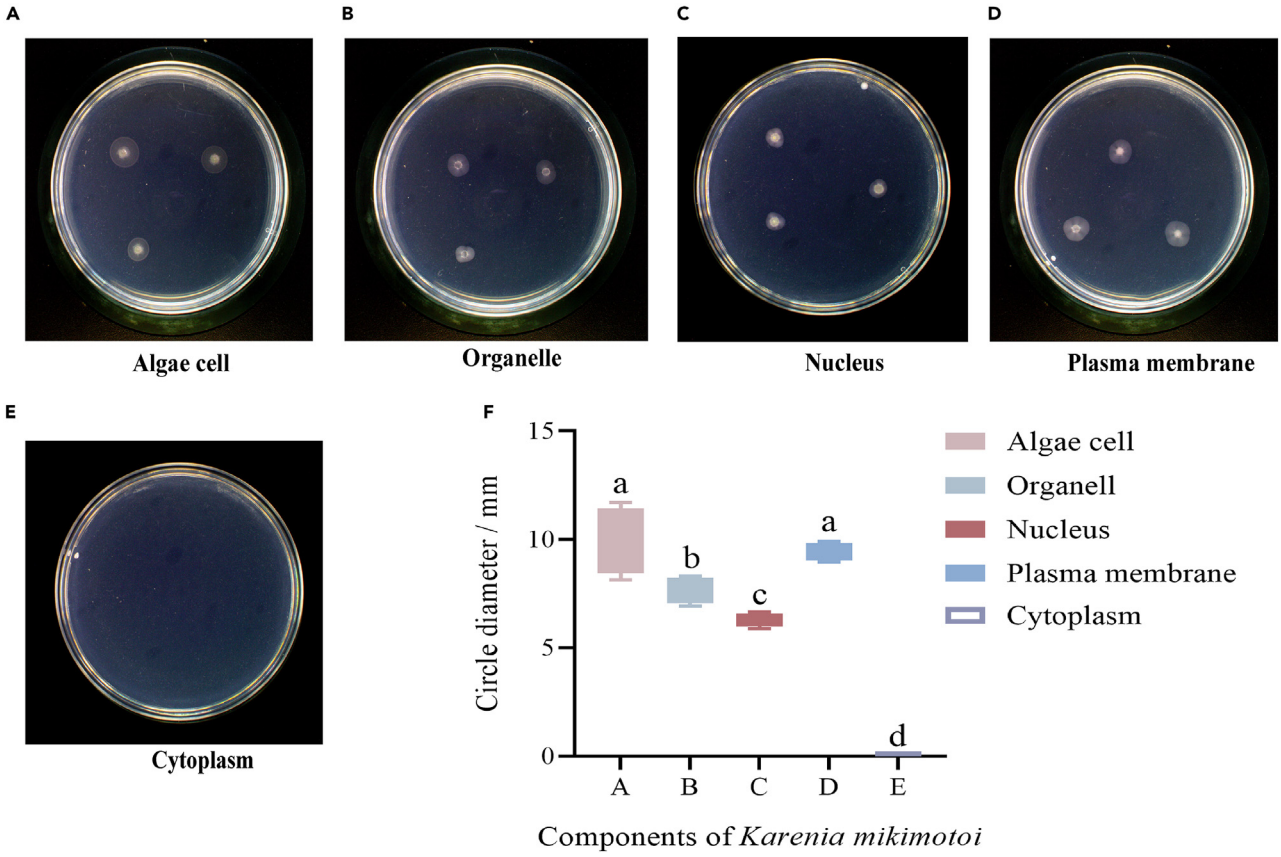

Figure 3. Chemotactic responses of ACE001 toward various components of algal cells

(A) Chemotaxis of ACE001 toward intact algal cells.

(B) Chemotaxis of ACE001 toward algal organelles.

(C) Chemotaxis of ACE001 toward algal nuclei.

(D) Chemotaxis of ACE001 toward the algal plasma membrane.

(E) Chemotaxis of ACE001 toward the algal cytoplasm.

(F) Diameter of the chemotactic circles formed by ACE001 in response to different components of algal cells. Data are presented as mean ± standard deviation, with distinct letters indicating statistically significant differences between groups.

determined the concentrations of Chlorophyll *a* after 6, 12, and 18 h of co-culture. Our findings revealed a decrease in Chlorophyll *a* content at the three time points by 22.96%, 33.72%, and 49.71%, respectively, compared to the control group. Notably, the changes in Chlorophyll *a* were consistent with the observed reduction in algal cell numbers (Figure 5A).

Changes in reactive oxygen species content within algal cells during co-cultivation with ACE001

We hypothesized that the mechanism of algal cell death may be associated with oxidative damage induced by the bacteria. To test this, we measured the intracellular levels of reactive oxygen species (ROS) in the algal cells after 1, 9, and 15 h of co-culture. A positive control group was treated with H_2O_2, while a negative control group was treated with PBS. Our measurements revealed a significant increase in ROS within the algal cells after 1 h of co-culture. The levels of ROS continued to rise by the 9th hour and, although they declined by the 15th hour compared to the 9th hour, they remained significantly elevated compared to the negative control (Figure 5B).

Genome sequencing of ACE001

To further elucidate the algicidal mechanism of ACE001, we sequenced its genome. The raw data were deposited to NCBI in SRA (BioProject accession number: PRJNA807487). The genome of ACE001 consists of two chromosomes and one plasmid, with a total chromosome length of 5,301,554 base pairs (bp) and a GC content of 44.30%. The genome encodes 4,501 genes with biological functions, of which 2,712 genes were annotated to KEGG pathways, including Metabolism, Environmental Information Processing, and Cellular Processes, among others. Additionally, the genome of ACE001 was found to contain 43 rRNAs, 137 tRNAs, and 14 sRNAs (Figure 6). Utilizing the PHI and VFDB databases, we identified pathogen-host interaction factors and virulence factors present in ACE001. A total of 1,017 pathogen-host interaction

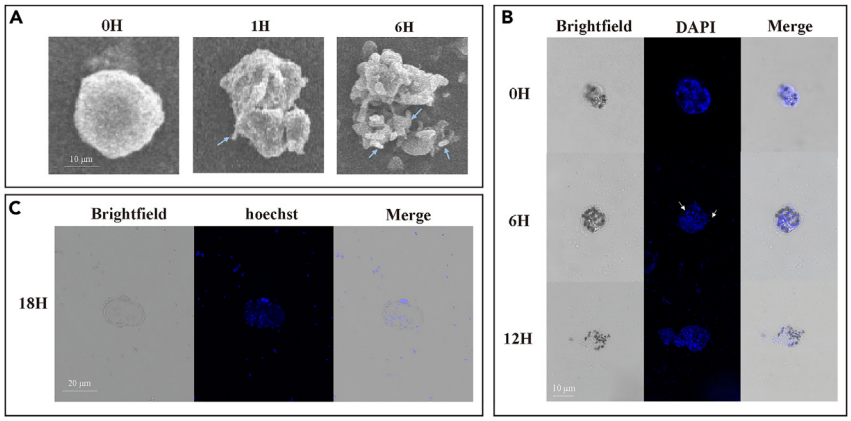

Figure 4. Morphological and structural alterations of *K. mikimotoi* during ACE001 infection

(A) Scanning electron microscopy (SEM) images of algal cells, with the blue arrow indicating ACE001.

(B) DAPI-stained algal cells visualized using confocal laser scanning microscopy (CLSM), where the white arrows denote bacterial presence.

(C) Hoechst 33342-stained algal cells observed via CLSM.

factors were identified, such as *luxO*, *leuO*, *vexB*, *cspB*, *aphB*, *cspV*, *phoP*, *phoQ*, and *VprA* (Table S1); 172 virulence factors were identified, including *tadA*, *fleQ*, *gspD*, *epsC*, *rmlA*, *htpB*, *mshB*, *cheV*, and *flgC* (Table S2). Enrichment analysis of the virulence genes revealed that most are implicated in bacterial pathogenic processes toward their hosts, such as Bacterial leaf blight, Salmonellosis, Septicemia, Nosocomial infections, and Infections (Figure S2). As previously confirmed in our study, chemotactic motility is crucial for the virulence of ACE001. During genomic analysis, we identified structural genes involved in the biosynthesis of the flagellum of ACE001. Moreover, the strain possesses multiple chemoreceptors and several signal transducers, with 48 genes annotated to the Bacterial chemotaxis pathway (Figure S3), indicating the strain's ability to respond chemotactically to attractants or repellents. These features may enable the planktonic ACE001 cells to navigate through the marine environment, locate nutrient-rich algal cells, and engage in directed swimming. The genome of the ACE001 strain also harbors various analysis systems, including the Type VI secretion system (T6SS), which are multifunctional bacterial weaponry capable of delivering effector molecules into a range of target cells. Given the contact-dependent bactericidal action of ACE001, it is plausible that these secretion systems play a significant role in its algicidal process. Furthermore, multiple two-component systems were identified in the genome, which are well-known for their role in recognizing environmental signals and stimuli. This may hold significant imply-cations for further research into the environmental adaptability of the ACE001 strain and the environmental drivers of virulence regulation.

Dual RNA-seq analysis of the interaction between ACE001 and *K. mikimotoi*

To explore the molecular biological processes underlying the interaction between ACE001 and *K. mikimotoi*, we conducted a dual RNA-seq analysis to simultaneously examine the gene expression patterns of both ACE001 and *K. mikimotoi* during the algicidal process. The raw data were deposited to NCBI in SRA (BioProject accession number: PRJNA1106094). Initially, we employed principal component analysis (PCA) to compare the samples and assess the variability and similarity among them. As depicted (Figure S4), the prokaryotic samples had contributions of 88.4% for PC1 and 10.9% for PC2, while the eukaryotic samples had contributions of 89.8% for PC1 and 6.7% for PC2. Intra-group variations were minimal, whereas inter-group differences were pronounced, indicating satisfactory reproducibility.

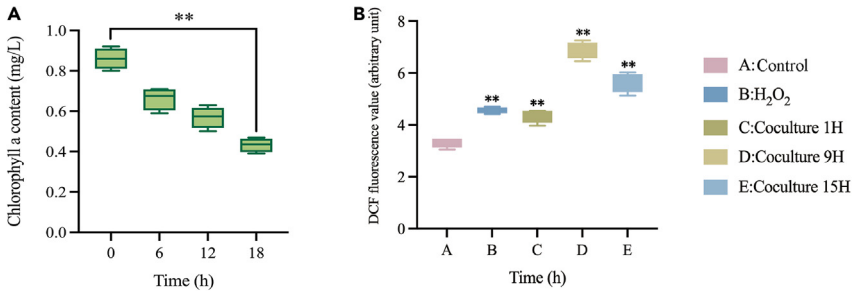

Figure 5. Impact of ACE001 on pigment and reactive oxygen species (ROS) levels in *K. mikimotoi* cells

(A) Variations in Chlorophyll *a* content in algal cells following co-culture with ACE001.

(B) Changes in ROS levels in algal cells post co-culture. Data are expressed as mean ± standard deviation. Significance levels are indicated as $p < 0.05$ (*), $p < 0.01$ (**).

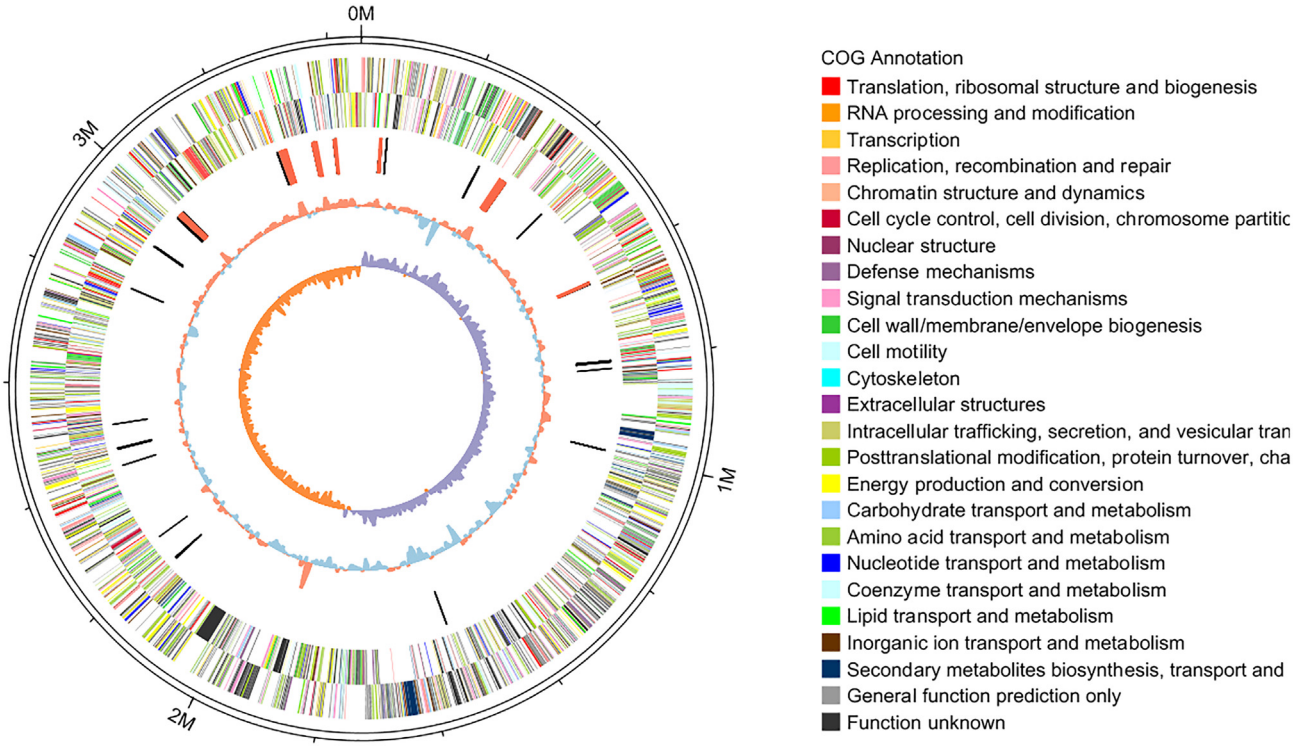

Figure 6. Genomic characteristics of ACE001

The circular diagram represents the genome of ACE001, organized from outer to inner layers: genome size scale (each segment corresponds to 5 kB); forward and reverse coding sequences (CDS), color-coded according to different COG functional classifications; repetitive sequences; tRNA (blue) and rRNA (purple); as well as GC content and GC skew plots.

To ensure the accuracy of the transcriptomic sequencing data, we randomly selected several upregulated and downregulated differentially expressed genes from the transcriptomes of both *V. coralliirubri* and *K. mikimotoi* for validation by qRT-PCR. The results demonstrated that the relative expression trends of these genes were largely consistent with those observed in the transcriptomic sequencing, confirming the accuracy of the dual RNA-seq findings (Figure S5).

In *K. mikimotoi*, a total of 12,176 genes were significantly upregulated, and 4,176 genes were significantly downregulated during the algicidal process (Figure 7A), which were annotated to biological processes, molecular functions, and cellular components (Figure S6). Within biological processes, the most annotated were cellular and metabolic processes, with 1,095 upregulated and 8,285 downregulated genes annotated to cellular processes, and 808 downregulated and 7,556 upregulated genes annotated to metabolic processes. In terms of molecular functions, the most annotated were catalytic activity, with 7,143 upregulated and 834 downregulated genes; binding, with 5,569 upregulated and 1,337 downregulated genes; and transporter activity, with 1,805 upregulated and 237 downregulated genes. In cellular components, the most annotated were cellular anatomical entities, including 5,255 upregulated and 603 downregulated genes. Among the 12,176 upregulated genes, the gene with the most significant change was Unigene0099712 ($log_2FC = 12.73$), annotated in KEGG as related to genetic information processing and in GO as related to ribosome constitution. Among the 4,176 downregulated genes, the gene with the most significant change was Unigene0063254 ($log_2FC = -15.19$), annotated in KEGG as related to metabolism and in GO as related to aerobic respiration in cells. As shown in Figure 7B, based on KEGG enrichment analysis, we screened genes involved in Plant-pathogen interaction, transport and catabolism, and signal transduction, hoping to find clues related to the death of *K. mikimotoi* cells. Three hours after bacterial stress on *K. mikimotoi* cells, genes involved in Plant-pathogen interaction, such as *hsp90*, *cpk30*, *cpk17*, *cpk22*, *phkg2*, *mpk15*, and *mpk1*, were downregulated, while genes involved in transport and catabolism, such as *tor*, *xdh*, *arfgef1*, *fadD15*, *fadN*, and *dnaK*, were significantly upregulated. Genes involved in signal transduction, such as *CAM1*, *mpk15*, *mpk1*, and *cml5*, were significantly downregulated, while *luxQ*, *dhkJ*, *phoB*, *ndk*, and *copA* were significantly upregulated. The differential expression of these genes provides clues to the mechanism of *K. mikimotoi* cell death. According to the dual RNA-seq results, a total of 483 genes in ACE001 were significantly upregulated, and 2,439 genes were significantly downregulated during the algicidal process (Figure 8A), which were annotated to biological processes, molecular functions, and cellular components (Figure S7). In biological processes, 1,514 significantly downregulated genes were annotated to cellular processes, 1,340 to metabolic processes, and 1,453 to single-organism processes. In molecular functions, 1,272 significantly downregulated genes were annotated to catalytic activity, and 1,142 to binding. In cellular components, 1,033 downregulated genes were annotated to the cell, and 1,033 to the cell part. Among the 483 upregulated genes, the gene with the most significant change was MID13_22490

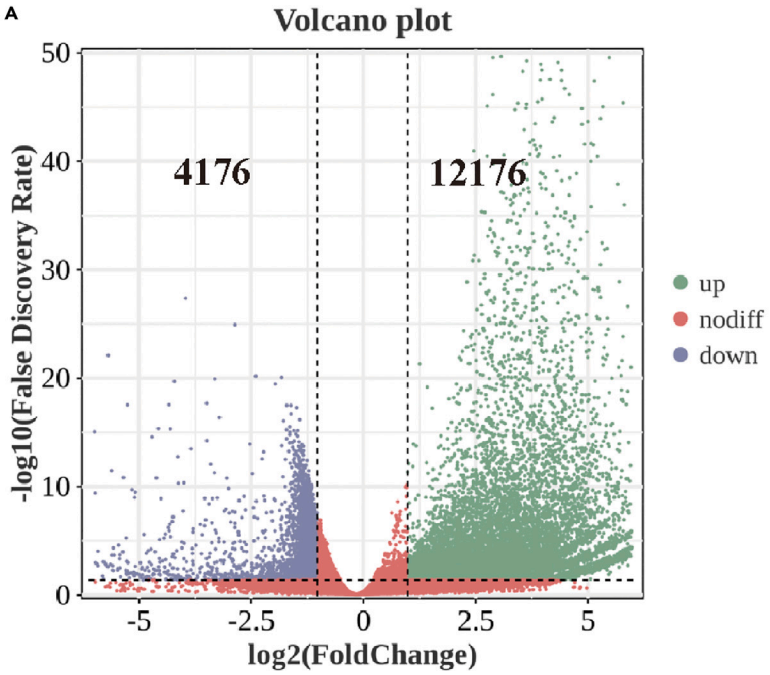
A
Volcano plot
4176
12176
up
nodiff
down
-log10(False Discovery Rate)
log2(FoldChange)
50
40
30
20
10
0
-5
-2.5
0
2.5
5

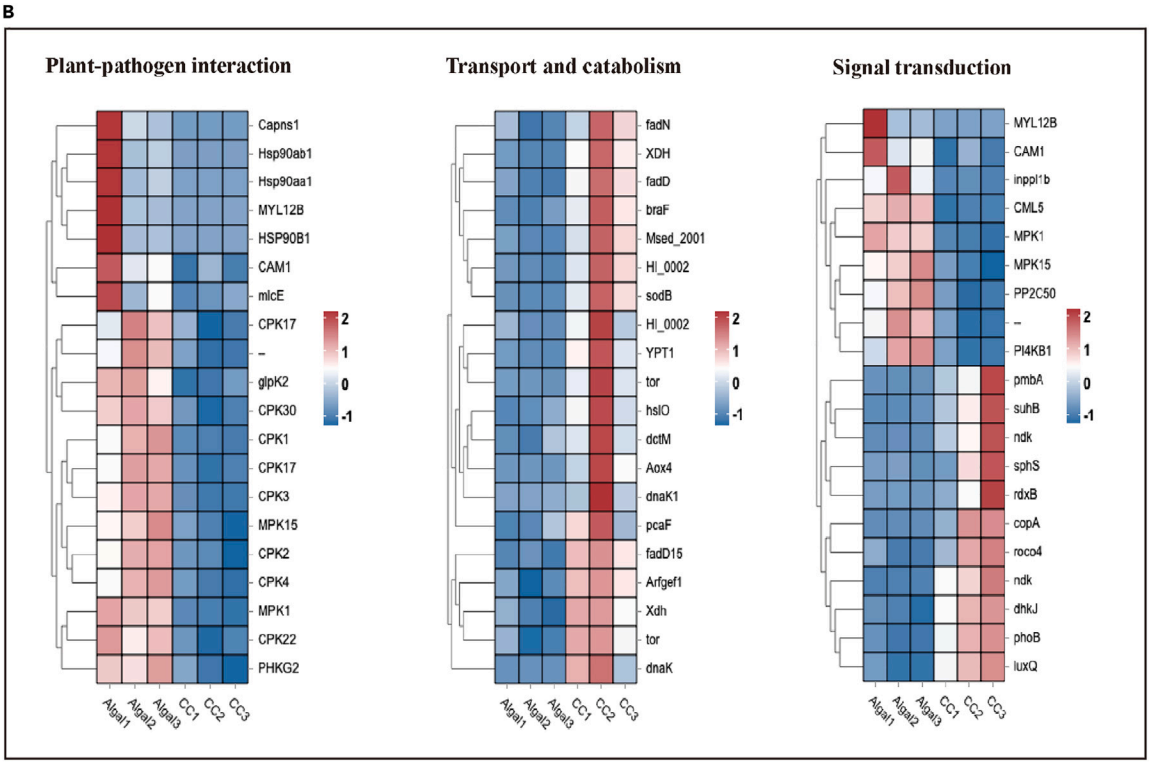
B
Plant-pathogen interaction
Capns1
Hsp90ab1
Hsp90aa1
MYL12B
HSP90B1
CAM1
mlcE
CPK17
–
glpK2
CPK30
CPK1
CPK17
CPK3
MPK15
CPK2
CPK4
MPK1
CPK22
PHKG2
Algal1
Algal2
Algal3
CC1
CC2
CC3
Transport and catabolism
fadN
XDH
fadD
braF
Msed_2001
HI_0002
sodB
HI_0002
YPT1
tor
hslO
dctM
Aox4
dnaK1
pcaF
fadD15
Arfgef1
Xdh
tor
dnaK
Signal transduction
MYL12B
CAM1
inppl1b
CML5
MPK1
MPK15
PP2C50
–
PI4KB1
pmbA
suhB
ndk
sphS
rdxB
copA
roco4
ndk
dhkJ
phoB
luxQ
2
1
0
-1

Figure 7. Gene expression modulation in *K. mikimotoi* post ACE001 infection

(A) Volcano plot illustrating gene expression changes in *K. mikimotoi* following ACE001 infection, with green dots indicating up-regulated genes, purple dots indicating down-regulated genes, and red dots denoting genes with no significant change. Smaller false discovery rates (FDR) indicate more significant differences.

(B) Differentially expressed genes associated with plant-pathogen interactions, transport and catabolism, and signal transduction pathways in *K. mikimotoi* after ACE001 infection. Red denotes up-regulated differentially expressed genes, while blue represents down-regulated genes.

(log_2FC = 11.76), predicted to be a permease component of the bacterial ABC transporter system. The permease component refers to substances such as peptides, proteins, and other macromolecules that bind to ABC transporter proteins and are then transported into or out of the cell. MID13_22490 showed a significant upregulation during the algicidal process, suggesting it may play an important role in the bacterium-algae interaction. MID13_03740, annotated as a protein containing the DUF3149 domain, showed a significant downregulation. The DUF3149 domain, typically ranging from 100 to 150 amino acids in length, is an "orphan" domain whose biological function and mechanism of action are not yet fully understood. The DUF3149 domain usually presents as a compact spherical structure with strong stability, thus being related to protein stability and folding. Additionally, the DUF3149 domain can work in conjunction with other domains to participate in complex biological processes. Although MID13_03740 was significantly downregulated during the algicidal process, the specific biological function of this gene and its role in the process remain unclear due to the lack of research on proteins containing the DUF3149 domain.

As depicted in Figure 8B, based on KEGG enrichment analysis, we screened differentially expressed genes related to bacterial secretion and chemotaxis. Notably, *gspE*, *tatC*, *glyS*, and *acul* were significantly upregulated, while *ddpD*, *phoQ*, *amy*, *avtA*, *tatA*, and *gspC* were significantly downregulated. Interestingly, genes associated with the Type VI secretion system (T6SS), such as *vgrG*, *hcp*, *dotU*, *clpV*, and *lip*, showed significant downregulation during the algicidal process. In addition, the Sec secretion system exhibited heightened activity, with the significant upregulation of *gspL* and *gspE*. The T6SS and Sec secretion systems are systems used by bacteria to transfer effector molecules to the external environment. The T6SS is a complex protein complex capable of directly injecting toxins or enzymatic molecules produced by bacteria into other cells, which can disrupt the host's cellular structure or interfere with normal physiological functions. The T6SS plays a significant role in bacterial interactions, pathogen infection of hosts, and bacterial adaptation to the environment. In this study, the T6SS was significantly suppressed, which may represent an energy-saving measure and suggests that the T6SS was not involved in the algicidal activity of ACE001. The Sec system is a complex protein machinery that is the primary secretion system for transporting unfolded bacterial proteins across the cytoplasmic membrane to the outside of the cell. This system relies on signal peptides to identify the correct protein transport complex targets and helps bacteria combat environmental stress. Exploration of the algicidal mechanisms involving the Sec secretion system is still in its infancy. Therefore, we selected *secY* and *yidC*, two genes with the most significant upregulation in the Sec secretion system, to construct knockout strains to investigate the role of the bacterial Sec secretion system in the algicidal process.

The Sec secretion system plays a key role in the algicidal process

In this study, we successfully constructed knockout and complemented strains for *yidC* and *secY* (Figures S8 and S9) and determined their growth curves. The results showed that compared to the wild type, the growth rate of the knockout strains was not significantly altered, remaining largely consistent with the wild-type growth rate, with no marked differences (Figure 9A). By co-culturing the wild type, Δ*yidC*, and C-Δ*yidC* strains of ACE001 at a concentration of 3×10^5 cfu/mL with *K. mikimotoi*, we assessed the impact of the absence of *yidC* and *secY* on the algicidal efficacy of ACE001. After 6 h of co-culture, the algicidal rates for the wild type, Δ*yidC*, and C-Δ*yidC* were 49.2%, 14.5%, and 27.2%. After 18 h of co-culture, the algicidal rates for the wild type, Δ*yidC*, and C-Δ*yidC* were 75.4%, 34.6%, and 62.6%, respectively. Similarly, after 6 h of co-culture, the algicidal rates for the wild type, Δ*secY*, and C-Δ*secY* were 49.2%, 15.1%, and 25.5%, respectively. After 18 h of co-culture, the algicidal rates for the wild type, Δ*secY*, and C-Δ*secY* were 75.4%, 36.4%, and 56.2%. It was observed that in all co-culture groups, the reduction in algal cell numbers was slower when co-cultured with the knockout strains (Figure 9B). Over time, the algicidal rate of the knockout strains was significantly lower than that of the wild type and complemented strains. During the co-culture process, the algicidal efficiency of the complemented strains was intermediate between that of the knockout and wild-type strains. These results indicate that the absence of *yidC* and *secY* significantly impacts the algicidal effect of ACE001. We also measured the impact of different strains on the Chlorophyll *a* content in *K. mikimotoi* after 6, 12, and 18 h of co-culture. The content of Chlorophyll *a* within the algal cells co-cultured with the wild type rapidly decreased over a short period (Figure 9C). After 18 h of co-culture with the wild type, the Chlorophyll *a* content in the algal cells decreased to 0.46 mg/L. The Chlorophyll *a* content in the cells co-cultured with Δ*secY* and C-Δ*secY* was 0.56 mg/L and 0.42 mg/L, respectively, and with Δ*yidC* and C-Δ*yidC* was 0.57 mg/L and 0.42 mg/L, respectively. Overall, the absence of *yidC* and *secY* significantly reduced the impact of ACE001 on the Chlorophyll *a* content in *K. mikimotoi*.

DISCUSSION

Previous research has revealed two primary modes of algicidal action by bacteria: direct (contact-mediated) and indirect algicidal modes [19,20]. The direct mode occurs only upon direct contact between bacterial and algal cells. For instance, Caiola et al. isolated a *Bdellovibrio*-like bacterium from the green alga *Microcystis aeruginosa*, which invades algal cells and resides between the cell wall and plasma membrane, dissolving the cells by degrading their structures.[20] Currently, more research has focused on the indirect algicidal mode, where bacterial strains secrete extracellular metabolites into the environment. These metabolites subsequently enter algal cells and exert toxic effects, establishing an indirect algicidal mode without the need for direct contact between bacteria and algae.[21] For example, during co-culture with

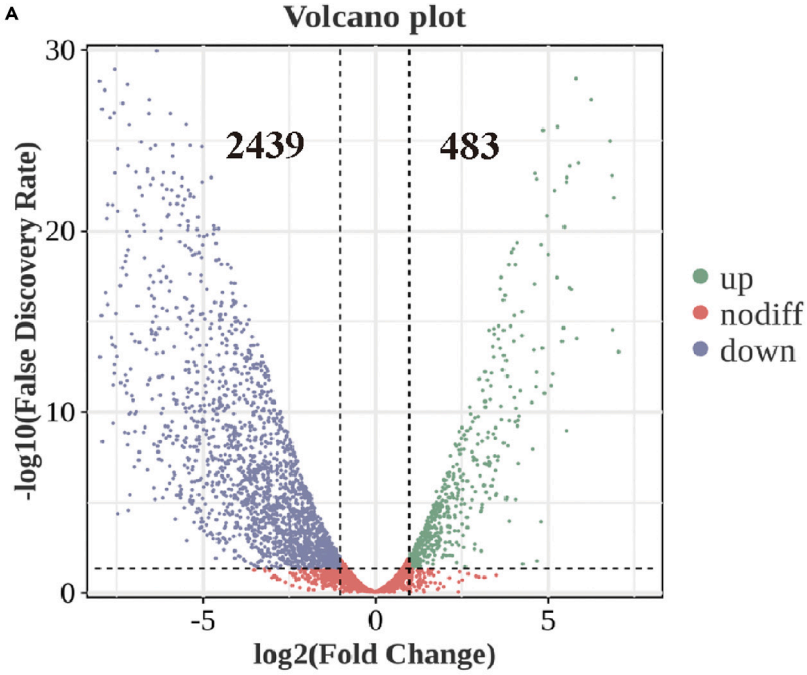
A
Volcano plot
2439
483
-log10(False Discovery Rate)
log2(Fold Change)
up
nodiff
down

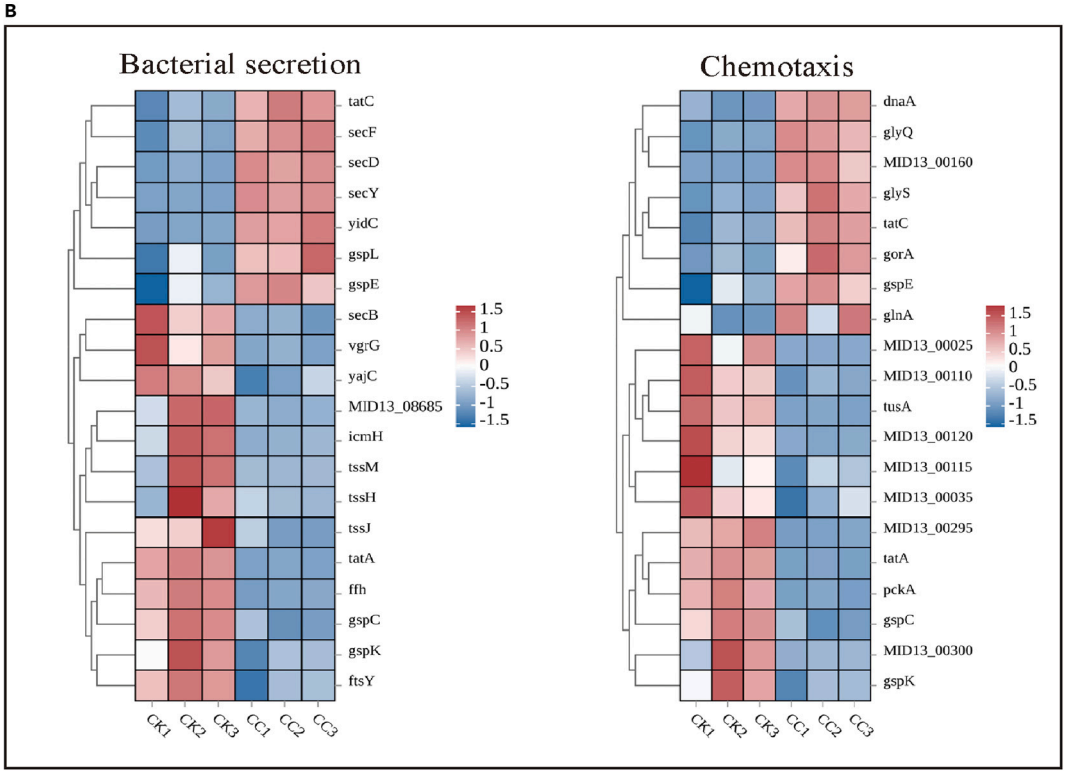
B
Bacterial secretion
tatC
secF
secD
secY
yidC
gspL
gspE
secB
vgrG
yajC
MID13_08685
icmH
tssM
tssH
tssJ
tatA
ffh
gspC
gspK
ftsY
CK1
CK2
CK3
CC1
CC2
CC3
Chemotaxis
dnaA
glyQ
MID13_00160
glyS
tatC
gorA
gspE
glnA
MID13_00025
MID13_00110
tusA
MID13_00120
MID13_00115
MID13_00035
MID13_00295
tatA
pckA
gspC
MID13_00300
gspK

Figure 8. Significant shifts in ACE001 gene expression patterns during the algal-killing process

(A) Volcano plot of differential gene expression across ACE001 samples, with green dots indicating up-regulated genes, purple dots for down-regulated genes, and red dots for non-differential genes. A smaller FDR signifies more pronounced differences.

(B) Differentially expressed genes in bacterial secretion and chemotaxis pathways of ACE001 during algal lethality. Up-regulated differentially expressed genes are shown in red, and down-regulated genes in blue.

the brown tide alga *Aureococcus anophagefferens*, the bacterium *Microbulbifer* YX04 continuously accumulates algicidal substances,[22] with the algicidal rate peaking (93.2%) after 60 h of bacterial-algal co-culture. Both direct and indirect algicidal bacteria have shown tremendous potential in controlling harmful algal blooms. Reports have shown that the *Pseudoalteromonas* genus can efficiently kill algae, with the addition of 1% volume of *Pseudoalteromonas* FDHY-M22 achieving an algicidal rate of 98.17% after 12 h of co-culture with *K. mikimotoi*[19]. Jeong-Dong Kim et al. isolated a strain of *Pseudoalteromonas haloplanktis* (AFMB-08041) from the marine environment, which demonstrated an algicidal rate of 94.5% against the harmful dinoflagellate *Prorocentrum minimum*.[23] In comparison, the ACE001 bacterial culture obtained in this study showed an algicidal rate of 95.2% after 24 h of co-culture with *K. mikimotoi*, confirming its high algicidal activity.

In our study, the supernatant of the *V. coralliirubri* ACE001 culture exhibited negligible algicidal activity, leading to our preliminary conclusion that ACE001 exerts its algicidal effect through direct contact with algal cells. When *K. mikimotoi* cells were separated from ACE001 by the dialysis bag and direct contact was prevented, the algal cells did not undergo death. This confirms that direct contact between the algal cells and the bacterial cells is a necessary condition to trigger the algicidal effect. Therefore, the algicidal mode of action of ACE001 is classified as direct algicidal activity. Prior to this, there have been reports confirming that bacteria dissolve *K. mikimotoi* through direct contact.[24] However, there is currently no in-depth report on the molecular mechanism by which bacteria kill *K. mikimotoi* through contact.

Interestingly, when co-cultivated with larger algae such as *Porphyra yezoensis*, ACE001 did not exhibit algicidal effects, demonstrating the highly specific selectivity of its algicidal action (data not shown). Considering the characteristics exhibited by ACE001, we hypothesize that it may utilize chemotactic movement to selectively target and contact specific algal cells. This is similar to reports on other contact mediated algicidal bacteria. For instance, Sonnenschein et al. conducted an in-depth study on *Aeromonas hydrophila* HP15 and the diatom *Thalassiosira weissflogii*. They discovered that HP15 is chemotactic toward *T. weissflogii* and identified a gene cluster associated with chemotaxis, which they mutagenized to create mutant strains. The results indicated that the Δ*cheA* and Δ*cheB* mutants showed defects in motility and a decrease in their ability to attach to *T. weissflogii*, highlighting the crucial role of chemotaxis in the bacterium-algae interaction process. In light of these findings, we investigated the chemotactic capability of ACE001 toward *K. mikimotoi* using a swarm motility assay. Our results revealed that ACE001 displays significant chemotaxis toward *K. mikimotoi*, aligning with the observed phenomenon of direct contact-mediated algicidal activity. In further research, we isolated and extracted various cellular fractions of *K. mikimotoi* and assessed their chemoattractant properties to ACE001. The experimental findings suggest that the cell membrane of *K. mikimotoi* exerts a potent chemoattractant effect on ACE001. Notably, the strongest chemotactic response was observed toward the algal cells and their membranes, indicating that certain proteins or lipids on the cell membrane of *K. mikimotoi* may possess a potent attractant for ACE001. Further research will be instrumental in identifying the specific inducers on the cell membrane of *K. mikimotoi* that guide the chemotactic behavior of ACE001.

Algal cells in aquatic environments are rich in dissolved organic matter (DOM), which can attract bacteria through chemotaxis. For instance, studies have confirmed that dimethylsulfoniopropionate (DMSP) serves as a chemoattractant between algae and bacteria,[25,26] suggesting that chemotaxis may act as a bridge in the algae-bacteria relationship. Bidle and colleagues have shown that the degradation of diatom frustules following cell death is associated with bacterial attachment.[27] Haiko[28] and others have reported that bacterial attachment is related to flagella, with flagellin proteins potentially acting as adhesins and also participating in the pathogenesis process as part of lipid rafts. It is evident that algal inducers are highly diverse, which may underlie the specificity of algicidal bacteria. In the present study, we found that ACE001 exhibits a strong chemotactic response to the cell membrane of *K. mikimotoi*, which we speculate may be due to proteins or lipids on the algal cell membrane attracting ACE001. However, the exact inducers remain to be identified. Future research will be dedicated to elucidating the components of the chemoattractants from *K. mikimotoi* and the specific molecular mechanisms by which ACE001 senses environmental chemical signals. For instance, we have identified 1,018 pathogen-host interaction factors and 172 virulence factors within the genome of the ACE001 strain, which are important clues for dissecting the virulence of the ACE001 strain. Among these, we discovered multiple two-component systems in the genome of ACE001. These systems are well-known for their role in recognizing environmental stimuli, which may be significant for further understanding the environmental sensing and adaptation capabilities of the ACE001 strain.[29]

Chloroplasts are the basis for photosynthesis in microalgae, and damage to these organelles can directly lead to the inhibition of the algal photosynthetic system, thereby affecting the growth and survival of the algae. Current research on the response of the photosynthetic system of microalgae during the algicidal process primarily focuses on changes in the content of Chlorophyll *a*. In the present study, the content of Chlorophyll *a* within *K. mikimotoi* cells continuously decreased with the duration of bacterial infection, indicating that the chloroplast structure may have been damaged under the action of ACE001, severely affecting the functionality of the photosynthetic system.[30]

When algal cells are subjected to external stimuli, an excessive amount of ROS can be produced. Excessive ROS can be toxic to algal cells.[31] Under conditions of stress, the intracellular content of ROS increases. When the stress is mild, the cell's own antioxidant system can promptly neutralize the reactive oxygen.[32] However, when the stress is severe, the ROS generated exceeds the cell's capacity to eliminate it, leading to the accumulation of ROS within the cell. We measured the ROS content in *K. mikimotoi* cells at three time points following treatment with ACE001 and observed a significant rise in ROS levels after 1 h of co-culture compared to the negative control. This indicates that

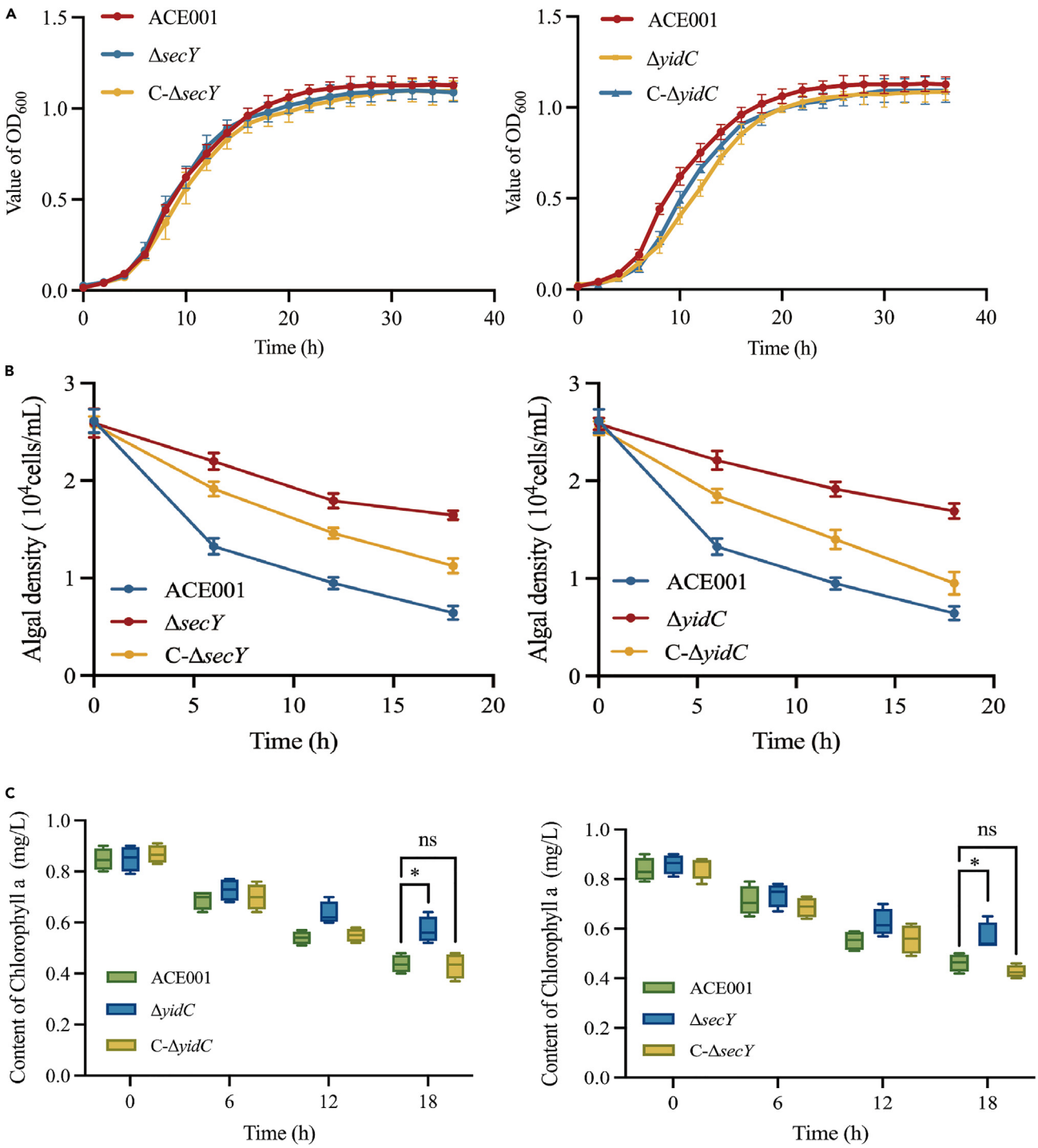

Figure 9. Impact of *secY* and *yidC* deletions on ACE001 virulence

(A) Growth curves for ACE001, Δ*secY*, Δ*yidC*, C-Δ*secY*, and C-Δ*yidC*.

(B) Algicidal efficiency of ACE001, Δ*secY*, Δ*yidC*, C-Δ*secY*, and C-Δ*yidC*.

(C) Changes in Chlorophyll *a* levels in algal cells post co-culture. Data are presented as mean ± standard deviation. $p < 0.05$ is indicated by *.

when *K. mikimotoi* cells are stressed by the bacterium ACE001, a robust oxidative stress response can occur rapidly, inflicting severe cellular damage on the algae. It has been confirmed in multiple species that an increase in ROS levels can trigger mechanisms such as autophagy and programmed cell death.[33] Therefore, we hypothesize that ROS may be a critical signal initiating cell death in *K. mikimotoi*.

We also examined the interaction between ACE001 and *K. mikimotoi* under confocal microscopy and SEM. The blue fluorescence within the cells appeared fragmented and disordered. In conjunction with the characteristics of organelle and nuclear disruption and dissolution, we postulate that the algal cells underwent necrosis under the influence of ACE001.

To further explore the algicidal mechanism of ACE001, we conducted a simultaneous analysis of gene expression in both ACE001 and *K. mikimotoi* using dual RNA-seq. During the algicidal process, we observed a significantly higher number of upregulated genes compared to downregulated ones in *K. mikimotoi*. The upregulated genes were predominantly enriched in metabolic pathways. We hypothesize that this may be an early response of *K. mikimotoi* to infection, where the synthesis of secondary metabolites is increased to enhance the algal cells' stress resistance in a changing environment. Previous reports have indicated that plant cells can produce secondary metabolites under stressful conditions to repel or attract biotic stressors, thereby protecting the plants from the harm caused by these stressors.[34]

We conducted a KEGG enrichment analysis to identify differentially expressed genes involved in Plant-pathogen interaction, transport and catabolism, and signal transduction in *K. mikimotoi*, with the aim of uncovering clues related to the death of algal cells. Notably, within the Plant-pathogen interaction pathway, we observed significant downregulation of the CPK genes, including *CPK17*, *CPK30*, *CPK1*, *CPK2*, *CPK3*, and *CPK4*, following infection. Calcium-dependent protein kinases (CPKs) are a class of specialized calcium signal sensors, composed of a multi-gene family of serine/threonine protein kinases, predominantly found in plants and microalgae.[22] These kinases can sense changes in extracellular calcium ion concentrations, bind to calcium ions, undergo conformational changes, and release auto-inhibitory domains, thereby activating the kinase. Activated CPKs transmit calcium signals to downstream targets through substrate phosphorylation, initiating a cascade of intracellular signaling pathways that ultimately regulate plant growth and development or responses to environmental stimuli. Studies have shown that plant cells can induce the CPK signaling pathway in response to biotic stress, including oxidative and hormonal signals.[35] *CPK17* negatively regulates plant metabolism by reducing the activity of enzymes in sugar and nitrogen metabolic pathways,[36] while glutathione helps to eliminate ROS toxicity generated under stress.[37] The downregulation of CPK expression may represent an early attempt by algal cells to counteract the rapid increase in intracellular ROS levels during bacterial stress, which aligns with our observations of a surge in reactive oxygen species during the initial stages of bacterio-algal interaction. Furthermore, we observed significant downregulation of *MPK1* and *MPK15* post-infection. Mitogen-activated protein kinases (MAPKs) are highly conserved serine/threonine protein kinases that are widely present in cascade reaction pathways in eukaryotic organisms. Their expression is regulated by reactive oxygen, hormones, and other factors, and they can phosphorylate a variety of substrates, including protein kinases and cytoskeleton-related proteins, playing a crucial role in plant stress response. Research has indicated that under certain conditions, plant cells can downregulate stress-resistant genes to better adapt to specific environmental pressures.[38] The downregulation of *MPK1* and *MPK15* may be a strategy employed by algal cells to conserve energy and better adapt to the environmental stress imposed by external bacterial challenges.

Within the transport and catabolism pathway, the TOR (Target of Rapamycin) gene demonstrated significant upregulation following infection. TOR, a serine/threonine protein kinase, is highly conserved across eukaryotes and plays a pivotal role in integrating various nutrients and growth factors to regulate multiple biological processes, including protein translation, metabolism, and autophagy.[39] An increasing body of research indicates that TOR is a key regulator of mitochondrial function and is intimately linked with redox metabolism in both lower and higher eukaryotes.[40] The TOR kinase targets an essential modulator of autophagy, providing a tunable autophagic response based on the cell's metabolic state.[41] Upregulation of TOR signifies that the cell has received sufficient nutritional signals, which can suppress the expression of autophagy-related genes and thus inhibit the onset of autophagy. Under normal growth conditions, basal autophagy rates serve as a quality control mechanism to maintain cellular homeostasis and longevity.[42] However, in response to energy stress, autophagic flux increases significantly, generating synthetic precursors to facilitate cellular adaptation and survival.[43] Autophagy, a primary process for the recycling of large amounts of proteins and organelles within cells under extracellular or intracellular stress, is a highly conserved intracellular degradation pathway in eukaryotic organisms and plays a crucial role in growth, development, aging, and responses to environmental stresses.[44] Cellular autophagy is closely associated with plants' defense against pathogen (viral, bacterial, fungal) invasion, participating in the regulation of basal defense and immune or disease-related cell death. The mode of action varies with the type of pathogen and the mode of invasion, especially under adverse conditions. For instance, studies have shown that autophagy can help plant cells eliminate damaged organelles and protein aggregates, maintaining intracellular stability. The initiation of autophagy mechanisms allows plants to control the dedifferentiation of the vascular sheath or xylem parenchyma cells, promoting xylem proliferation and enhancing resistance to vascular diseases.[45] Upon pathogen invasion, cells can effectively trigger autophagy,[46] which, through hyper-sensitive response-induced programmed cell death, prevents further pathogen infection.[47]

We observed a rapid increase in cellular ROS shortly after the contact of ACE001 with algal cells. Traditionally, ROS have been perceived as toxic substances that only cause cellular damage. However, recent studies have shown that ROS, acting as signaling molecules, are also involved in various physiological processes, including cell proliferation, differentiation, and apoptosis, playing a crucial regulatory role in plant growth and development, stress adaptation, and programmed cell death.[48] Excess ROS generated under stress conditions can often lead to cellular damage, and cells must invoke more active mechanisms to eliminate damaged components and maintain ROS under control. Autophagy is a primary defense mechanism for the degradation of oxidized molecules and may also eliminate organelles producing ROS under certain conditions. Chloroplasts are a major source of ROS in plants and algae. Izumi et al. found that chloroplast components can be degraded through the process of autophagy under carbon starvation induced by darkness.[37–39] In light of the aforementioned results of decreased pigment content in algal cells following bacterial stress, we hypothesize that *K. mikimotoi* likely produced a large amount of ROS in the chloroplasts upon direct contact with ACE001, which then induced the autophagic mechanism to clear ROS-generating organelles, such as chloroplasts, leading to the dissolution and fragmentation of organelles. This is consistent with the disrupted and disorganized

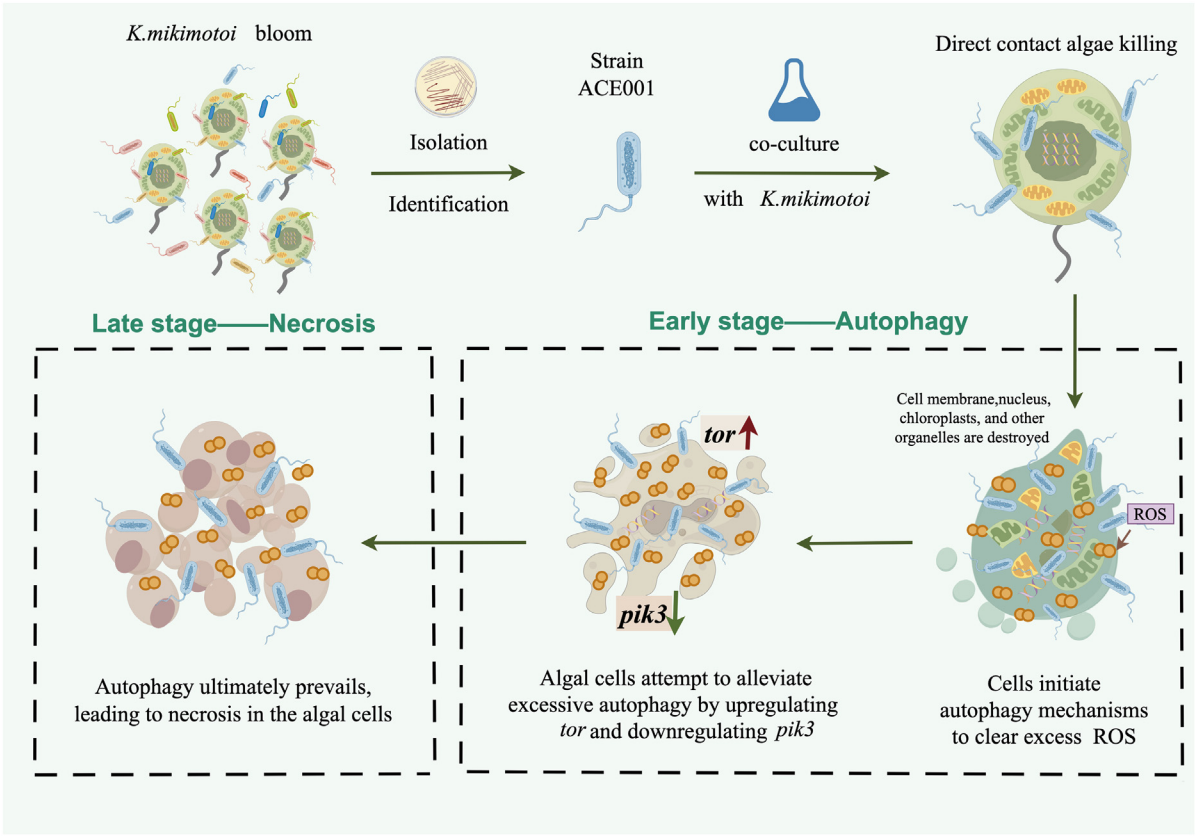

Figure 10. Schematic representation of the mechanism through which ACE001 induces *K. mikimotoi* cell death

internal structure of algal cells observed under confocal microscopy. Following autophagy, the algal cells may attempt to activate TOR to suppress excessive autophagy and alleviate the degradation of intracellular organelles. Concurrent with the upregulation of the tor gene expression, a significant downregulation of *pik3* was observed. The *pik3* gene encodes Phosphoinositide 3-kinase (PI3K), an important signaling enzyme that plays a key role in numerous biological processes, including cell growth, differentiation, survival, migration, and metabolism. In plant cells, PI3K is primarily involved in regulating processes such as cell wall formation, cell division, and cell death, and it also positively regulates the autophagic process in plant cells.[49] We speculate that the downregulation of PI3K is another strategy employed by algal cells to counteract the autophagy induced by ACE001. Studies have found that autophagy works in concert with lysosomal degradation to facilitate cell death. Samara et al. showed that excessive autophagosome formation is induced early in the process of necrotic cell death in *Caenorhabditis elegans*, where autophagy contributes to cellular destruction during necrosis.[50] Therefore, we hypothesize that after the production of a large amount of ROS, the cells initiate an autophagic mechanism to degrade organelles such as chloroplasts. Although the algal cells attempt to alleviate the overactive autophagy by upregulating TOR and downregulating PI3K, autophagy ultimately prevails, leading to necrosis in the algal cells (Figure 10).

Our findings revealed that nearly all genes associated with chemotaxis and secretion in the bacteria showed differential expression after 3 h of stress imposed on *K. mikimotoi* cells, further validating our hypothesis. Interestingly, the Type VI secretion system (T6SS), a critical bacterial nano-weapon, exhibited extremely low activity during the interaction. Genes such as *vgrG*, *hcp*, *lip*, *icmF*, *dotU*, and *clpV* were all significantly downregulated. This could be attributed to an unknown inhibitory mechanism of *K. mikimotoi* against the T6SS, or it may suggest that the T6SS is not essential for the algicidal process. To conserve limited energy, ACE001 may have chosen to keep the T6SS in a dormant state. In contrast, we observed significant upregulation of most genes within the Sec secretion system, such as *gspL*, *gspE*, *secY*, and *yidC*. Collectively, it appears that ACE001 has economized on the energy demands of the T6SS and redirected it toward the efficient operation of the Sec secretion system. The Sec secretion system is a vital pathway for the translocation of membrane proteins in bacteria and is known to control the export of various virulence factors, including exotoxins, pili, adhesins, and invasins.[40] To date, there have been no studies or reports on the functionality of the Sec secretion system in algicidal bacteria. In light of this, we constructed knockout strains for two genes, *secY* and *yidC*, which were significantly upregulated in the Sec secretion system, with the aim of investigating the role of the Sec system in the algicidal process.

In the present study, we co-cultivated the Δ*secY*, Δ*yidC*, C-Δ*secY*, and C-Δ*yidC* strains with *K. mikimotoi* and observed a significant reduction in the algicidal efficiency of the knockout strains. This efficiency was restored upon the complementation of *secY* and *yidC* in the

respective Δ*secY* and Δ*yidC* strains. The *secY* and *yidC* knockout mutations also diminished the impact of ACE001 on the content of Chlorophyll *a*. These findings suggest that *secY* and *yidC* are implicated in the regulation of virulence and the infectious process of ACE001 toward *K. mikimotoi*.

Taken together, this study delves into the intricate interplay between bacteria and algae, elucidating the mechanism by which ACE001 exerts its lethal effects on *K. mikimotoi*.

Limitations of the study

Despite the significant findings, our research is not without limitations. Firstly, while we have established the potent chemotactic response of ACE001 toward *K. mikimotoi*, the specific inducers on the cell membrane of *K. mikimotoi* remain elusive and require further clarification. Future endeavors will focus on dissecting the molecular mechanisms underlying algal chemotaxis, particularly seeking insights centered around the extensive pathogen-host interactions and virulence factors within the ACE001 genome. Secondly, in the realm of reported bactericidal research, the majority of bacterial algicidal modes are indirect,[51] with bacteria exerting their effects on algal cells through the secretion of extracellular metabolic products.[52] Algicidal substances often include pigments,[53] peptides,[54] proteins, and antibiotics. Given the vast array and structural similarities of bacterial metabolites, their separation and purification present considerable challenges. The contact-mediated algicidal mode of ACE001 poses unique challenges and opportunities in elucidating its mechanism of action. Subsequent research will be dedicated to characterizing the algicidal effectors of ACE001, laying a theoretical foundation for strategies in the control of harmful algal blooms.

RESOURCE AVAILABILITY

Lead contact

For more information and correspondence, please contact Prof. Lixing Huang, lixinghuang@jmu.edu.cn.

Materials availability

This study did not generate any new reagents.

Data and code availability

- All data supporting the findings of this study are provided within the article and its supplemental information section. The genome of *V. coralliirubri* ACE001 has been deposited in SRA (BioProject accession number: PRJNA807487). Raw data of the dual RNA-seq analysis has been deposited in SRA (BioProject accession number: PRJNA1106094).
- This article does not report the original code.
- Any additional information required to reanalyze the data reported in this article is available from the lead contact upon reasonable request.

ACKNOWLEDGMENTS

The author(s) declare financial support was received for the research, authorship, and/or publication of this article. This work was supported by the National Natural Science Foundation of China (No. 32173016) and the Natural Science Foundation of Fujian Province (No. 2022J02044).

AUTHOR CONTRIBUTIONS

JY, JW, QG, and LX conceived the experiments. All authors assisted in the collection and interpretation of data. JY, LH, and QY wrote the article. All authors contributed to the article and approved the submitted version.

DECLARATION OF INTERESTS

The authors declare that the research was conducted in the absence of any commercial or financial relationships that could be construed as a potential conflict of interest.

STAR★METHODS

Detailed methods are provided in the online version of this paper and include the following:

- KEY RESOURCES TABLE
- EXPERIMENTAL MODEL AND STUDY PARTICIPANT DETAILS
  - Bacterial cultures
  - Algal cultures
- METHOD DETAILS
  - Phylogenetic tree construction
  - Algicidal efficiency of various concentrations of ACE001
  - Algicidal efficiency of ACE001's filtered supernatant
  - Dialysis bag isolation experiment
  - Chemotactic activity assay of ACE001
  - Scanning electron microscope observation
  - Confocal laser scanning microscope observation
  - Genomic sequencing of ACE001
  - Photosynthetic pigments detection in algal cells

- ROS content detection in algal cells
- Dual RNA-seq analysis
- qRT-PCR analysis of gene expression
- Construction of *yidC* and *secY* mutants of ACE001
- Complementation of the Δ*secY* and Δ*yidC* strains
- Determination of ACE001 growth curves

- QUANTIFICATION AND STATISTICAL ANALYSIS

SUPPLEMENTAL INFORMATION

Supplemental information can be found online at https://doi.org/10.1016/j.isci.2024.111254.

Received: May 7, 2024
Revised: June 14, 2024
Accepted: October 23, 2024
Published: October 28, 2024

REFERENCES

1. Patel, S.S., Lovko, V.J., and Lockey, R.F. (2020). Red Tide: Overview and Clinical Manifestations. J. Allergy Clin. Immunol. Pract. *8*, 1219–1223.
2. Xiao, X., Li, C., Huang, H., and Lee, Y.P. (2019). Inhibition effect of natural flavonoids on red tide alga Phaeocystis globosa and its quantitative structure-activity relationship. Environ. Sci. Pollut. Res. Int. *26*, 23763–23776.
3. Lee, H.J., Shin, M., Kim, M.S., Kim, T., Lee, K.M., Park, N.B., Lee, J.C., and Lee, C. (2023). Removal of the red tide dinoflagellate Cochlodinium polykrikoides using chemical disinfectants. Water Res. *242*, 120230.
4. Park, J., Church, J., Son, Y., Kim, K.T., and Lee, W.H. (2017). Recent advances in ultrasonic treatment: Challenges and field applications for controlling harmful algal blooms (HABs). Ultrason. Sonochem. *38*, 326–334.
5. Liao, X., Wang, X., Zhao, K., and Zhou, M. (2009). Photocatalytic inhibition of cyanobacterial growth using silver-doped TiO2 under UV-C light. J. Wuhan Univ. Technol. -Mat. Sci. Edit. *24*, 402–408.
6. Sun, H.Y., Zhang, Y., Chen, H.R., Hu, C.X., Li, H., and Hu, Z.L. (2016). Isolation and characterization of the marine algicidal bacterium Pseudoalteromonas S1 against the harmful alga Akashiwo sanguinea. Mar. Biol. *163*, 1–8.
7. Li, Y., Lei, X., Zhu, H., Zhang, H., Guan, C., Chen, Z., Zheng, W., Fu, L., and Zheng, T. (2016). Chitinase producing bacteria with direct algicidal activity on marine diatoms. Sci. Rep. *6*, 21984.
8. Grasso, C., Pokrzywinski, K., Wang, Y., & Coyne, K. DinoSHIELD: A Slow-Release Natural Algicide Produced by Shewanella sp. IRI-160 for Management of Red-Tide. In SETAC North America 41st Annual Meeting. SETAC.
9. Coyne, K.J., Wang, Y., and Johnson, G. (2022). Algicidal Bacteria: A Review of Current Knowledge and Applications to Control Harmful Algal Blooms. Front. Microbiol. *13*, 871177.
10. Li, D.X., Zhang, H., Chen, X.H., Xie, Z.X., Zhang, Y., Zhang, S.F., Lin, L., Chen, F., and Wang, D.Z. (2018). Metaproteomics reveals major microbial players and their metabolic activities during the blooming period of a marine dinoflagellate Prorocentrum donghaiense. Environ. Microbiol. *20*, 632–644.
11. Ding, N., Gao, P., Xu, D., Xing, E., Li, Y., Sun, L., Wang, R., and Zhang, W. (2022). Characterization and algicidal activity of bacteria from the phycosphere of the harmful alga Karenia mikimotoi. Braz. J. Microbiol. *53*, 891–901.
12. Shi, X., Liu, L., Li, Y., Xiao, Y., Ding, G., Lin, S., and Chen, J. (2018). Isolation of an algicidal bacterium and its effects against the harmful-algal-bloom dinoflagellate *Prorocentrum donghaiense* (Dinophyceae). Harmful Algae *80*, 72–79.
13. Zhang, F., Ye, Q., Chen, Q., Yang, K., Zhang, D., Chen, Z., Lu, S., Shao, X., Fan, Y., Yao, L., et al. (2018). Algicidal Activity of Novel Marine Bacterium Paracoccus sp. Strain Y42 against a Harmful Algal-Bloom-Causing Dinoflagellate, Prorocentrum donghaiense. Appl. Environ. Microbiol. *84*, e01015-18.
14. Roth, P.B., Twiner, M.J., Mikulski, C.M., Barnhorst, A.B., and Doucette, G.J. (2008). Comparative analysis of two algicidal bacteria active against the red tide dinoflagellate Karenia brevis. Harmful Algae *7*, 682–691.
15. Hare, C.E., Demir, E., Coyne, K.J., Craig Cary, S., Kirchman, D.L., and Hutchins, D.A. (2005). A bacterium that inhibits the growth of Pfiesteria piscicida and other dinoflagellates. Harmful Algae *4*, 221–234.
16. Ding, N., Du, W., Feng, Y., Song, Y., Wang, C., Li, C., Zheng, N., Gao, P., and Wang, R. (2021). Algicidal activity of a novel indigenous bacterial strain of Paracoccus homiensis against the harmful algal bloom species, Karenia mikimotoi. Arch. Microbiol. *203*, 4821–4828.
17. Zheng, N., Ding, N., Gao, P., Han, M., Liu, X., Wang, J., Sun, L., Fu, B., Wang, R., and Zhou, J. (2018). Diverse algicidal bacteria associated with harmful bloom-forming *Karenia mikimotoi* in estuarine soil and seawater. Sci. Total Environ. *631–632*, 1415–1420.
18. Mayali, X., and Azam, F. (2004). Algicidal bacteria in the sea and their impact on algal blooms 1. J. Eukaryot. Microbiol. *51*, 139–144.
19. Shi, X., Zou, Y., Zheng, W., Liu, L., Xie, Y., Ma, R., and Chen, J. (2022). A Novel Algicidal Bacterium and Its Effects against the Toxic Dinoflagellate *Karenia mikimotoi* (Dinophyceae). Microbiol. Spectr. *10*, e0042922.
20. Caiola, M.G., and Pellegrini, S. (1984). Lysis of Microcystis aeruginosa (Kütz.) by Bdellovibrio-like bacteria 1. J. Phycol. *20*, 471–475.
21. Guan, C., Guo, X., Li, Y., Zhang, H., Lei, X., Cai, G., Guo, J., Yu, Z., and Zheng, T. (2015). Photoinhibition of Phaeocystis globosa resulting from oxidative stress induced by a marine algicidal bacterium Bacillus sp. LP-10. Sci. Rep. *5*, 17002.
22. Zhu, X., Chen, S., Luo, G., Zheng, W., Tian, Y., Lei, X., Yao, L., Wu, C., and Xu, H. (2022). A Novel Algicidal Bacterium, Microbulbifersp. YX04, Triggered Oxidative Damage and Autophagic Cell Death in *Phaeocystis globosa*, Which Causes Harmful Algal Blooms. Microbiol. Spectr. *10*, e0093421.
23. Kim, J.D., Kim, J.Y., Park, J.K., and Lee, C.G. (2009). Selective control of the Prorocentrum minimum harmful algal blooms by a novel algal-lytic bacterium *Pseudoalteromonas haloplanktis* AFMB-008041. Mar. Biotechnol. *11*, 463–472.
24. Shi, J., Wang, W., Wang, F., Lei, S., Shao, S., Wang, C., Li, G., and An, T. (2023). Efficient inactivation of harmful algae K. mikimotoi by a novel algicidal bacterium via a rare direct contact pathway: Performances and mechanisms. Sci. Total Environ. *892*, 164401.
25. Barak-Gavish, N., Frada, M.J., Ku, C., Lee, P.A., DiTullio, G.R., Malitsky, S., Aharoni, A., Green, S.J., Rotkopf, R., Kartvelishvily, E., et al. (2018). Bacterial virulence against an oceanic bloom-forming phytoplankter is mediated by algal DMSP. Sci. Adv. *4*, eaau5716.
26. Smriga, S., Fernandez, V.I., Mitchell, J.G., and Stocker, R. (2016). Chemotaxis toward phytoplankton drives organic matter partitioning among marine bacteria. Proc. Natl. Acad. Sci. USA *113*, 1576–1581.
27. Bidle, K.D., and Azam, F. (1999). Accelerated dissolution of diatom silica by marine bacterial assemblages. Nature *397*, 508–512.
28. Haiko, J., and Westerlund-Wikström, B. (2013). The role of the bacterial flagellum in adhesion and virulence. Biology *2*, 1242–1267.
29. Liao, B., Ye, X., Chen, X., Zhou, Y., Cheng, L., Zhou, X., and Ren, B. (2021). The two-component signal transduction system and its regulation in *Candida albicans*. Virulence *12*, 1884–1899.
30. Zhang, H., Wang, H., Zheng, W., Yao, Z., Peng, Y., Zhang, S., Hu, Z., Tao, Z., and Zheng, T. (2017). Toxic Effects of Prodigiosin Secreted by *Hahella* sp. KA22 on Harmful

Alga *Phaeocystis globosa*. Front. Microbiol. *8*, 999.

31. Burnham, J.C., Collart, S.A., and Daft, M.J. (1984). Myxococcal predation of the cyanobacterium Phormidium luridum in aqueous environments. Arch. Microbiol. *137*, 220–225.
32. Ding, N., Wang, Y., Chen, J., Man, S., Lan, F., Wang, C., Hu, L., Gao, P., and Wang, R. (2021). Biochemical and Physiological Responses of Harmful *Karenia mikimotoi* to Algicidal Bacterium *Paracoccus homiensis* O-4. Front. Microbiol. *12*, 771381.
33. Miki, H., Uehara, N., Kimura, A., Sasaki, T., Yuri, T., Yoshizawa, K., and Tsubura, A. (2012). Resveratrol induces apoptosis via ROS-triggered autophagy in human colon cancer cells. Int. J. Oncol. *40*, 1020–1028.
34. Al-Khayri, J.M., Rashmi, R., Toppo, V., Chole, P.B., Banadka, A., Sudheer, W.N., Nagella, P., Shehata, W.F., Al-Mssallem, M.Q., Alessa, F.M., et al. (2023). Plant Secondary Metabolites: The Weapons for Biotic Stress Management. Metabolites *13*, 716.
35. Yip Delormel, T., and Boudsocq, M. (2019). Properties and functions of calcium-dependent protein kinases and their relatives in Arabidopsis thaliana. New Phytol. *224*, 585–604.
36. Almadanim, M.C., Alexandre, B.M., Rosa, M.T.G., Sapeta, H., Leitão, A.E., Ramalho, J.C., Lam, T.T., Negrão, S., Abreu, I.A., and Oliveira, M.M. (2017). Rice calcium-dependent protein kinase OsCPK17 targets plasma membrane intrinsic protein and sucrose-phosphate synthase and is required for a proper cold stress response. Plant Cell Environ. *40*, 1197–1213.
37. Hayat, S., Hayat, Q., Alyemeni, M.N., Wani, A.S., Pichtel, J., and Ahmad, A. (2012). Role of proline under changing environments: a review. Plant Signal. Behav. *7*, 1456–1466.
38. Wang, B., Zhang, H., Huai, J., Peng, F., Wu, J., Lin, R., and Fang, X. (2022). Condensation of SEUSS promotes hyperosmotic stress tolerance in Arabidopsis. Nat. Chem. Biol. *18*, 1361–1369.
39. Liu, Y., and Xiong, Y. (2022). Plant target of rapamycin signaling network: Complexes, conservations, and specificities. J. Integr. Plant Biol. *64*, 342–370.
40. Schieke, S.M., and Finkel, T. (2006). Mitochondrial signaling, TOR, and life span. Biol. Chem. *387*, 245–1361.
41. Vlahakis, A., Graef, M., Nunnari, J., and Powers, T. (2014). TOR complex 2-Ypk1 signaling is an essential positive regulator of the general amino acid control response and autophagy. Proc. Natl. Acad. Sci. USA *111*, 10586–10591.
42. Madeo, F., Tavernarakis, N., and Kroemer, G. (2010). Can autophagy promote longevity? Nat. Cell Biol. *12*, 842–846.
43. Onodera, J., and Ohsumi, Y. (2005). Autophagy is required for maintenance of amino acid levels and protein synthesis under nitrogen starvation. J. Biol. Chem. *280*, 31582–31586.
44. Qian, R., Zhao, H., Liang, X., Sun, N., Zhang, N., Lin, X., and Sun, C. (2022). Autophagy alleviates indium-induced programmed cell death in wheat roots. J. Hazard Mater. *439*, 129600.
45. Wang, F.X., Luo, Y.M., Ye, Z.Q., Cao, X., Liang, J.N., Wang, Q., Wu, Y., Wu, J.H., Wang, H.Y., Zhang, M., et al. (2018). iTRAQ-based proteomics analysis of autophagy-mediated immune responses against the vascular fungal pathogen Verticillium dahliae in Arabidopsis. Autophagy *14*, 598–618.
46. Liu, Y., Schiff, M., Czymmek, K., Tallóczy, Z., Levine, B., and Dinesh-Kumar, S.P. (2005). Autophagy regulates programmed cell death during the plant innate immune response. Cell *121*, 567–577.
47. Valmonte, G.R., Arthur, K., Higgins, C.M., and MacDiarmid, R.M. (2014). Calcium-dependent protein kinases in plants: evolution, expression and function. Plant Cell Physiol. *55*, 551–569.
48. Gechev, T.S., Van Breusegem, F., Stone, J.M., Denev, I., and Laloi, C. (2006). Reactive oxygen species as signals that modulate plant stress responses and programmed cell death. Bioessays *28*, 1091–1101.
49. Liu, F., Hu, W., Li, F., Marshall, R.S., Zarza, X., Munnik, T., and Vierstra, R.D. (2020). AUTOPHAGY-RELATED14 and Its Associated Phosphatidylinositol 3-Kinase Complex Promote Autophagy in Arabidopsis. Plant Cell *32*, 3939–3960.
50. Samara, C., Syntichaki, P., and Tavernarakis, N. (2008). Autophagy is required for necrotic cell death in Caenorhabditis elegans. Cell Death Differ. *15*, 105–112.
51. Zhang, H., An, X., Zhou, Y., Zhang, B., Zhang, S., Li, D., Chen, Z., Li, Y., Bai, S., Lv, J., et al. (2013). Effect of oxidative stress induced by Brevibacterium sp. BS01 on a HAB causing species–Alexandrium tamarense. PLoS One *8*, e63018.
52. Huang, L., Hu, J., Su, Y., Qin, Y., Kong, W., Ma, Y., Xu, X., Lin, M., and Yan, Q. (2015). Identification and characterization of three Vibrio alginolyticus non-coding RNAs involved in adhesion, chemotaxis, and motility processes. Front. Cell. Infect. Microbiol. *5*, 56.
53. Nakashima, T., Miyazaki, Y., Matsuyama, Y., Muraoka, W., Yamaguchi, K., and Oda, T. (2006). Producing mechanism of an algicidal compound against red tide phytoplankton in a marine bacterium gamma-proteobacterium. Appl. Microbiol. Biotechnol. *73*, 684–690.
54. Park, S.C., Lee, J.K., Kim, S.W., and Park, Y. (2011). Selective algicidal action of peptides against harmful algal bloom species. PLoS One *6*, e26733.
55. Wang, C., Xu, Y., Gu, H., Luo, Z., Luo, Z., and Su, R. (2024). Potential geographical distribution of harmful algal blooms caused by the toxic dinoflagellate *Karenia mikimotoi* in the China Sea. Sci. Total Environ. *906*, 167741.
56. Hou, S., Shu, W., Tan, S., Zhao, L., and Yin, P. (2016). Exploration of the antioxidant system and photosynthetic system of a marine algicidal Bacillus and its effect on four harmful algal bloom species. Can. J. Microbiol. *62*, 49–59.
57. Kanehisa, M., and Goto, S. (2000). KEGG: Kyoto Encyclopedia of Genes and Genomes. Nucleic Acids Res. *28*, 27–30.
58. Karna, S.L.R., Nguyen, J.Q., Evani, S.J., Qian, L.W., Chen, P., Abercrombie, J.J., Sebastian, E.A., Fourcaudot, A.B., and Leung, K.P. (2020). T3SS and alginate biosynthesis of *Pseudomonas aeruginosa* impair healing of infected rabbit wounds. Microb. Pathog. *147*, 104254.
59. Du, Z., Zhang, M., Qin, Y., Zhao, L., Huang, L., Xu, X., and Yan, Q. (2022). The role and mechanisms of the two-component system EnvZ/OmpR on the intracellular survival of *Aeromonas hydrophila*. J. Fish. Dis. *45*, 1609–1621.
60. Love, M.I., Huber, W., and Anders, S. (2014). Moderated estimation of fold change and dispersion for RNA-seq data with DESeq2. Genome Biol. *15*, 550.
61. Robinson, M.D., McCarthy, D.J., and Smyth, G.K. (2010). edgeR: a Bioconductor package for differential expression analysis of digital gene expression data. Bioinformatics *26*, 139–140.
62. Xiu, L., Wu, Y., Lin, G., Zhang, Y., and Huang, L. (2024). Bacterial membrane vesicles: orchestrators of interkingdom interactions in microbial communities for environmental adaptation and pathogenic dynamics. Front. Immunol. *15*, 1371317.
63. Xu, K., Wang, Y., Yang, W., Cai, H., Zhang, Y., and Huang, L. (2022). Strategies for Prevention and Control of Vibriosis in Asian Fish Culture. Vaccines (Basel) *11*, 98.
64. Wang, J., Li, Q., and Huang, L. (2023). Effect of the zinc transporter ZupT on virulence mechanism of mesophilic Aeromonas salmonicida SRW-OG1. Anim. Res. One Health *1*, 1–13.

STAR★METHODS

KEY RESOURCES TABLE

REAGENT or RESOURCE	SOURCE	IDENTIFIER
Bacterial and virus strains		
Vibrio coralliirubri ACE001	This study	N/A
Biological samples		
Karenia mikimotoi	Obtained from Dr. Haifeng Gu of the Third Institute of Oceanography, Ministry of Natural Resources, China.	N/A
Chemicals, peptides, and recombinant proteins		
Marine Broth 2216 Agar	Difco	212185
f/2 medium	Guangyu	GY-M22-50
Chloramphenicol	Macklin	CAS#: 56-75-7
Tetracycline	Solarbio	CAS#: 64-75-5
Hoechst 33342	Solarbio	CAS#: YZM002032
Ampicillin	Solarbio	CAS#: 69-52-3
Kanamycin	Solarbio	CAS#: K8020-1
4′,6-diamidino-2-phenylindole (DAPI)	Life Technologies	CAS#: 28718-90-3
Critical commercial assays		
Minute™ Plant Plasma Membrane Protein Isolation Kit	Invent	CAS#: SM-005-P
Enhanced BCA Protein Assay Kit	Beyotime	CAS#: P0010
ROS assay kit	Nanjing Jiancheng	CAS#: E004-1-1
SYBR Green Supermix	Bio-Rad	CAS#: 1708882
EasyPure® Plasmid MiniPrep kit	TransGen	CAS#: EM101-02
Pfu PCR Master Mix kit	LABLEAD	CAS#: T0211
Deposited data		
The genome of *Vibrio coralliirubri* ACE001	This study	The raw data were deposited to NCBI in SRA (BioProject accession number: PRJNA807487).
dual RNA-seq analysis to simultaneously examine the gene expression patterns of both ACE001 and *K. mikimotoi* during the algicidal process.	This study	The raw data were deposited to NCBI in SRA (BioProject accession number: PRJNA1106094).
Software and algorithms		
SPASS 19.0	IBM	https://www.ibm.com/cn-zh/analytics/spss-statistics-software

EXPERIMENTAL MODEL AND STUDY PARTICIPANT DETAILS

Bacterial cultures

The strain *V. coralliirubri* ACE001 utilized in this study was isolated from the Dongshan sea area of Fujian Province during a red tide outbreak, wherein *K. mikimotoi* was identified as the predominant microalga responsible for the event. Following isolation and purification, the strain was cultured in 2216E medium at 28°C and agitated at 220 revolutions per minute (rpm) for 8 to 12 hours to ensure it reached the logarithmic growth phase. After cultivation, the bacterial culture was evenly mixed with a glycerol stock solution in a 1:1 ratio and subsequently stored at -80°C for long-term preservation.

Algal cultures

K. mikimotoi was obtained from Dr. Gu.[55] It was cultivated in a photo incubator at a temperature of 20°C, under a light intensity of 100 μmol photons/(m^2·s), with a 12-hour light:dark cycle. The algal cultures were grown in f/2 medium (Shanghai Guangyu Biological Technology Co., Ltd, China), prepared with natural seawater that was filtered through a 0.45 μm filter to remove bacterial contaminants, maintained at a temperature of 20 ± 1°C. Prior to the algicidal assays, the algal suspension was preconditioned with an antibiotic mixture to eliminate any potential bacterial presence in the growth environment. This antibiotic cocktail included ampicillin (200 mg/L), kanamycin (100 mg/L), and streptomycin (100 mg/L). The concentration of *K. mikimotoi* cells was then quantified using a hemocytometer and adjusted to a density of 1.5-3 × 10^4 cells/mL for subsequent experimental procedures. Before conducting the experiments, we verified the elimination of bacteria in the culture medium through plate culture and colony counting (Figure S10).

METHOD DETAILS

Phylogenetic tree construction

The 16S rDNA gene sequence of the *V. coralliirubri* ACE001 strain was analyzed using the EzTaxon-e database, revealing a similarity exceeding 99% with the 16S rDNA sequences of known *V. coralliirubri* species. For phylogenetic analysis, the 16S rDNA gene sequence of the ACE001 strain was subjected to a BLAST comparison in the NCBI database, with sequences from common Vibrio species selected as references. Using MEGA 7.0 software, a phylogenetic tree was constructed employing the Neighbor-Joining (NJ) method. The resulting sequence alignments were visualized using ClustalW, alongside the ESPript 3.x/ENDscript 2.x suite.

Algicidal efficiency of various concentrations of ACE001

ACE001 was inoculated into 100 mL of 2216E medium and cultured at 28°C with shaking at 220 rpm until the bacterial concentrations reached three gradient densities: 1.5×10^5, 3×10^5, and 3×10^6 cfu/mL. Subsequently, 2 mL aliquots of the ACE001 cultures at each concentration were added to 50 mL of 1×10^4 cells/mL *K. mikimotoi* algal suspension according to Shi et al.[19] A control was established by adding 2 mL of 2216E liquid medium to the algal suspension. Each treatment was performed in triplicate biological replicates, followed by co-cultivation for 24 hours. Thereafter, aliquots from the different treatment groups were taken and the algal cells were counted under an optical microscope using a hemocytometer. The inhibition rate (IR) was calculated using the following formula: IR(%) = (1−Ni/N0) × 100%, where IR represents the inhibition rate, N0 is the algal cell density in the control group, and Ni is the algal cell density in the experimental group.

Algicidal efficiency of ACE001's filtered supernatant

ACE001 was inoculated into 100 mL of 2216E medium and cultured at 28°C with shaking at 220 rpm until the concentration reached 3×10^5 cfu/mL. Subsequently, 2 mL of the bacterial culture was centrifuged at 4000 rpm for 10 minutes to collect the supernatant. The supernatant was then filtered through a 0.22 μm membrane filter to obtain a sterile filtered supernatant of ACE001. Aliquots of 2 mL from both the ACE001 bacterial culture and the sterile filtered supernatant were introduced into 50 mL of *K. mikimotoi* culture. A control was established by adding 2 mL of 2216E medium to the algal culture. Each treatment was carried out in triplicate biological replicates. At 6, 12, and 18 hours post co-cultivation, 100 μL samples were taken from the 50 mL algal-bacterial culture, and the algal cells were counted under an optical microscope to assess the algicidal rate across different treatment durations.

Dialysis bag isolation experiment

The bacterial culture of ACE001 was centrifuged at 5000 rpm for 5 minutes at room temperature to pellet the cells. The resulting bacterial pellet was subsequently washed twice with sterile f/2 medium. Following these washes, the pellet was resuspended in an equivalent volume of sterile f/2 medium. An aliquot of the resuspended bacterial solution was transferred into sterile dialysis bags at a concentration of 4% (v/v). These dialysis bags, containing the ACE001 culture, were submerged in a culture of *K. mikimotoi*. For comparison, dialysis bags filled with an equal volume of sterile f/2 medium served as a negative control and were also introduced into the algal culture. After 18 hours, the algicidal rate was determined using the methodology outlined in the previous section.

Chemotactic activity assay of ACE001

An 800 μL aliquot of the logarithmic phase culture of ACE001 was centrifuged at 5,000 rpm for 5 minutes. The supernatant was discarded, and the resulting pellet was washed twice with sterile f/2 medium. The bacteria were then resuspended in 800 μL of f/2 medium to create a bacterial suspension. A 0.18% agarose f/2 semi-solid medium was prepared, sterilized, and allowed to cool to room temperature. The bacterial suspension was subsequently mixed with the agarose medium, and the resultant mixture was poured into Petri dishes to form semi-solid agar plates. For the preparation of algal samples, 50 mL of *K. mikimotoi* culture was centrifuged at 3,500 rpm for 5 minutes and washed twice with sterile f/2 medium. The pellet was resuspended in 10 μL of sterile f/2 medium. The cellular membrane, organelles, nucleus, and cytoplasm of *K. mikimotoi* were isolated using the Minute™ Plant Plasma Membrane Protein Isolation Kit (Invent Biotechnology, USA). An aliquot of 2 μL of the algal cell suspension or various cellular components was dissolved in f/2 medium. Protein concentration was quantified using the Enhanced BCA Protein Assay Kit (Beyotime Biotechnology, China) and adjusted to a final concentration of 0.7 mg/mL. Equal volumes of these protein solutions were then spotted onto the prepared f/2 semi-solid agar plates. The plates were incubated at 28°C, and the development of chemotactic rings was assessed after overnight incubation.

Scanning electron microscope observation

Fifty milliliters of *K. mikimotoi* culture, as well as the co-cultures with bacterial strain ACE001 (at a concentration of 0.3×10^6 cfu/mL) for 1 hour and 6 hours, were centrifuged at 3500 rpm for 5 minutes. The resulting pellets were fixed in 2.5% glutaraldehyde at 4°C for 12 hours. Following the removal of the fixative, the samples were washed with phosphate-buffered saline (PBS) and subsequently fixed in a 1% osmium tetroxide solution for 1 hour. After osmium fixation, the samples were washed again with PBS. The samples underwent a graded series of ethanol solutions for dehydration, culminating in a 20-minute treatment with 100% ethanol. Finally, the samples were immersed in 100% ethanol and dried using a critical point dryer (Quorum K850). After drying, the samples were sputter-coated with gold using a scanning electron microscope (SEM) sputter coater (Hitachi MC1000) and subsequently examined under a scanning electron microscope (Hitachi SU3050).

Confocal laser scanning microscope observation

Following treatment with the ACE001 culture, algal cells were harvested at 6 and 12 hours. A 5 mL aliquot of the algal culture was centrifuged at 1000 rpm for 5 minutes to pellet the cells, which were subsequently washed with 1 mL of phosphate-buffered saline (PBS). To stain the nuclei, 200 μL of DAPI (4′,6-diamidino-2-phenylindole) (Solarbio, China) was added to the pellet. The samples were then incubated in the dark at room temperature for 5 minutes, followed by two washes with PBS, and resuspended in 1 mL of PBS. A small drop of the suspension was placed onto a microscope slide, covered with a coverslip, and examined using a confocal laser scanning microscope (CLSM, model Zeiss LSM 780) equipped with a 40× objective lens and a band-pass filter of 435-485 nm to observe DAPI fluorescence. Representative images were captured. For the samples treated with algicidal bacteria for 18 hours, the bacterial and algal cell cultures were processed as described above, with Hoechst 33342 (Solarbio, China) added for nuclear staining. The treated cells were observed, and representative images were obtained using the whole-slide imaging analysis platform MICA (Leica, Germany) under the same conditions.

Genomic sequencing of ACE001

Genomic DNA was extracted using the HiPure Bacterial DNA Extraction Kit (Magen, Guangzhou, China), adhering strictly to the manufacturer's protocols. The quality of the extracted DNA was evaluated utilizing Qubit (Thermo Fisher Scientific, Waltham, MA) and NanoDrop (Thermo Fisher Scientific, Waltham, MA) instruments. Genomic sequencing was conducted on the MinION Mk1B device employing the DNANK-RAD002 Rapid Sequencing Kit (Oxford Nanopore Technologies, ONT, USA), in accordance with the standard operating procedures outlined by ONT.

Qualified genomic DNA underwent random sonication, followed by end-repair, A-tailing, and adaptor ligation utilizing the NEBNext® MLtra™ DNA Library Prep Kit for Illumina (NEB, USA) as per the preparation guidelines. DNA fragments ranging from 300 to 400 bp in length were enriched via PCR. Subsequently, PCR products were purified using the AMPure XP system (Beckman Coulter, Brea, CA, USA), and library quality was assessed for size distribution using the 2100 Bioanalyzer (Agilent, Santa Clara, CA) and quantified through real-time PCR. Genome sequencing was performed on the Illumina Novaseq 6000 sequencer employing paired-end technology (PE 150).

Raw data from the Illumina platform were filtered using FASTP (version 0.20.0) according to established standards. The assembled contigs underwent further refinement with Pilon v1.22 to ensure high-quality genome assembly. A circular representation of the whole genome was generated utilizing Circos software. Coding sequences within the assembled genome were predicted using Prodigal software. The predicted gene sequences were aligned against functional databases, including COG (https://www.ncbi.nlm.nih.gov/research/cog-project/), KEGG (https://www.genome.jp/kegg/), Swiss-Prot (https://www.uniprot.org), and NR using BLAST to obtain functional annotations.

Based on the NR database alignment results, Blast2GO was employed for functional annotation against the Gene Ontology (GO). Furthermore, we conducted functional annotation with COG, enrichment analysis of KEGG metabolic pathways, and GO functional enrichment analysis. Finally, the predicted gene sequences were compared against functional databases, including the Pathogen-Host Interaction (PHI) database (http://www.phi-base.org) and the Virulence Factor Database (VFDB) (http://www.mgc.ac.cn/VFs/main.htm), to obtain corresponding annotation results.

Photosynthetic pigments detection in algal cells

Following treatment with the bacterial suspension for 0, 6, 12, and 18 hours, 20 mL aliquots of the *K. mikimotoi* culture were collected. The samples were centrifuged at 2000 rpm for 10 minutes at 20°C, after which the supernatant was discarded. Subsequently, 5 mL of 95% acetone was added, and the samples were extracted for 24 hours in a refrigerator at 4°C. The extracts were then centrifuged at 6000 rpm for 10 minutes at 20°C, and the supernatant was collected. The absorbance values at 665, 645, and 630 nm were measured using a visible spectrophotometer. The concentrations of Chlorophyll *a* was calculated using the following equations[56]:

$$C_{\text{Chlorophyll a}}\left(\text{mg}\cdot\text{L}^{-1}\right) = 11.6\times A_{665}\text{-}1.31\times A_{645}\text{-}0.14\times A_{630}$$

ROS content detection in algal cells

The ROS content in *K. mikimotoi* cells was quantified using a Reactive Oxygen Species Assay Kit provided by Nanjing Jiancheng Bioengineering Institute (China). In accordance with the manufacturer's protocol, algal cell suspensions were collected into 1.5 mL centrifuge tubes and washed twice with 0.01 M phosphate-buffered saline (PBS). The tubes were then centrifuged at 1000 rpm for 5 minutes to discard the supernatant. Subsequently, the cells were centrifuged again at 2000 rpm for 5 minutes to isolate the cell pellet. After two additional washes with 0.01 M PBS and re-centrifugation, the supernatant was removed, and the cells were resuspended in 1 mL of PBS. A ROS probe was

introduced to achieve a final concentration of 10 μM. For the negative control, an equal volume of PBS was substituted for the probe. In the positive control, a hydrogen donor, which induces ROS production, was added to the reaction mixture containing the probe at a concentration of 20 μM. The reaction systems were incubated at 37°C for 20 minutes, with intermittent mixing through inversion every 3-5 minutes. Following the incubation period, the cell suspensions were subjected to centrifugation at 1000 rpm for 5 minutes, and the supernatant was discarded. The cells were washed twice with PBS, and then the algal cells were recentrifuged at 1000 rpm for 5 minutes, collected, and resuspended in 1 mL of PBS. The ROS content was subsequently measured using flow cytometry (Beckman Coulter International Trade (Shanghai) Co., Ltd.).

Dual RNA-seq analysis

The *V. coralliirubri* ACE001 strain was cultured at 28°C with a shaking speed of 220 rpm until the bacterial suspension reached a concentration of 3×10^5 cfu/mL for subsequent use. Regarding the choice of bacterial concentration, our preliminary experiments obtained a half-lethal concentration of 1.5×10^5 cfu/mL. To ensure that the samples collected during the dual RNA-seq were in the most active stage of bacteria-algae interaction, we chose this bacterial concentration. The 1×10^4 cells/mL *K. mikimotoi* was co-cultured with the aforementioned bacterial suspension for 3 hours. Total RNA was extracted from the ACE001 culture, *K. mikimotoi* culture, and their co-culture system using the TRIzol method (Life Technologies, CA, USA). The dual RNA-seq analysis was then performed on the Illumina 6000 platform (Illumina, San Diego, CA, USA) at Guangzhou genedenovo Biotech Co., Ltd., with three biological replicates set for each group. To obtain high-quality sequencing data, the raw sequencing data were filtered,[57] and the reads were assembled using the Trinity software. The assembly completeness was assessed with the BUSCO software.[58] We employed the RSEM software[59] to calculate the gene expression levels in terms of FPKM (Fragments Per Kilobase of transcript per Million mapped reads) and performed a correlation analysis of the gene expression levels among samples. Differentially expressed genes (DEGs) for each sequencing sample were identified using the DESeq2 software,[60] with edgeR[61] used for differential expression analysis between two samples. The criteria for selecting significantly differentially expressed genes were: FDR (False Discovery Rate) < 0.05 & $|\log_2$ Fold Change$|$ > 1. Gene Ontology (GO) (http://www.geneontology.org/) enrichment analysis was conducted for both *V. coralliirubri* and *K. mikimotoi*, with GO functions with a corrected *p*-value of less than 0.05 considered significantly enriched. Corrected *p*-values of less than 0.05 for KEGG pathways are considered to be significantly enriched.[60] Based on the transcriptome data of *V. coralliirubri* and *K. mikimotoi*, we selected multiple genes, including upregulated, downregulated, and non-differentially expressed genes, for validation using the quantitative real-time PCR (qRT-PCR) technique.

qRT-PCR analysis of gene expression

qRT-PCR was performed using the QuantStudio 6 Flex system (Life Technologies, USA).[62,63] Primer sequences were designed with Primer Premier 5.0 software, and the specific primers employed in this study are detailed in Table S3. These primers were synthesized by Shanghai Sangon Biological Engineering Technology & Services Co., Ltd (China). The reaction mixture consisted of 10 μL per well (UltraFlux® i PCR 8-strip Low Profile 0.1 mL with individually attached flat caps) and included 5 μL of SYBR Green Supermix (Bio-Rad, USA), 0.25 μL of each forward and reverse primer, 0.5 μL of diluted template DNA, and 4 μL of nuclease-free water. The 16S rRNA gene and the GAPDH gene were utilized as endogenous reference genes for normalizing gene expression levels in *V. coralliirubri* and *K. mikimotoi*, respectively. Each treatment group was assessed in triplicate biological replicates, and relative gene expression levels were calculated using the $2^{-\Delta\Delta Ct}$ method.[64]

Construction of *yidC* and *secY* mutants of ACE001

Based on the gene sequences of *secY* and *yidC* from *V. coralliirubri*, homo-logous arm primers were designed using Snap Gene. The 5′ ends of these primers were homologous to 21 base pairs of the flanking regions immediately preceding and following the gene sequences targeted for deletion, while the 3′ ends were homologous to the termini of the kanamycin resistance gene. The primers utilized in this process are listed in Table S4 and were synthesized by Shanghai Sangon Biological Engineering Technology & Services Co., Ltd. Following the protocol outlined in the EasyPure® Plasmid MiniPrep kit manual provided by TransGen Biotech Co., Ltd. (China), the pet-28a+ plasmid was extracted from *E. coli*. Employing the aforementioned primers and adhering to the instructions of the 2× Pfu PCR Master Mix kit (LABLEAD Biotech, China), the pet-28a+ plasmid was subjected to PCR amplification to construct targeting fragments specific for *secY* and *yidC*, which included the kanamycin resistance. The plasmid PACYC184/red was conjugatively transformed into *V. coralliirubri* and cultured until the OD_{600} reached 0.3. The culture was then induced with 30 mmol/L L-arabinose to express the recombinase genes *exo*, *bet*, and *gam* carried by PACYC184/red. Subsequently, the linear targeting fragments excised from agarose were conjugatively transformed into *V. coralliirubri* containing PACYC184/red. Positive clones were selected using chloramphenicol and kanamycin, with the addition of L-arabinose for induction. Positive colonies were picked for PCR amplification and sequencing to verify the successful construction of the mutants.

Complementation of the Δ*secY* and Δ*yidC* strains

The complementation strains C-Δ*secY* and C-Δ*yidC* were constructed with modifications to the previously described methods.[58] C-Δ*secY*-F and C-Δ*secY*-R were primers used to amplify a 1335 bp full-length fragment of the *secY* gene from the genomic DNA of ACE001. The fragment and the plasmid pCM130/tac were digested with *BsrGI* HF and *NsiI* HF (New England Biolabs, USA), and the resulting fragments were ligated using T4 DNA ligase. The ligation products were then heat-shocked into competent *E. coli* DH5α, and successful complementation plasmids pCM130/tac-C-secY were selected on 2216E agar plates containing tetracycline (Tat, 10 μg/mL). The complementation strain

C-Δ*secY* was confirmed by PCR and sequencing. The complementation strain C-Δ*yidC* was constructed using an analogous method, with the primers C-Δ*yidC*-F and C-Δ*yidC*-R.

Determination of ACE001 growth curves

The ACE001 growth assay was performed with minor modifications to the previously established protocol.[59] Wild-type, knockout, and complemented strains were cultivated in 2216E medium at 28°C until an optical density at 600 nm (OD600) of approximately 0.5 was achieved. Subsequently, the bacterial cultures were diluted to an OD600 of about 0.2 and further diluted 105-fold with sterile fresh 2216E medium. Two hundred microliters of the diluted bacterial suspension were transferred into a 96-well plate, with an equivalent volume of 2216E medium added to the wells as a control group. The growth of ACE001 was monitored by measuring OD600 values hourly for 36 hours at 28°C using a Synergy H1 microplate reader (BioTek, USA). Eight biological replicates were conducted for each bacterial strain.

QUANTIFICATION AND STATISTICAL ANALYSIS

In the present study, data analysis was performed using SPSS software (version 19.0). Statistical results are reported as mean values ± standard deviation (Mean ± S.D.). Inter-group differences were evaluated using one-way analysis of variance (ANOVA) followed by Dunnett's multiple comparison test. A *p*-value of less than 0.05 was considered statistically significant. For Figure 1, each treatment underwent three biological replicates, with the algal solution counted using eight 100 μL aliquots. For Figures 2, 3, 4, and 5, each treatment consisted of three biological replicates. For Figures 7 and 8, three biological replicates were performed. For Figure 9, Growth curves were assessed with eight biological replicates per treatment, while chlorophyll content and algal cell counts post co-culture were measured with three biological replicates, utilizing eight counts of 100 μL aliquots.

Graphical representations, including bar graphs and line graphs, were generated using GraphPad Prism (version 8.0.2). All schematic diagrams in this article were created using FigDraw.